New result of $e^+e^- \to \pi^+\pi^-$ from CMD3 and its implication to $(g\text{-}2)_\mu$

B.Shwartz on behalf of CMD-3 collaboration

Budker Institute of Nuclear Physics, Novosibirsk,

Novosibirsk State University

$$\mathcal{H} = -\vec{\mu} \cdot \vec{B} - \vec{d} \cdot \vec{E}$$

Magnetic Dipole Moment $\vec{\mu} = g \left(\frac{q}{2m} \right) \vec{s}$

$$a = \left(\frac{\alpha}{2\pi} \right)$$

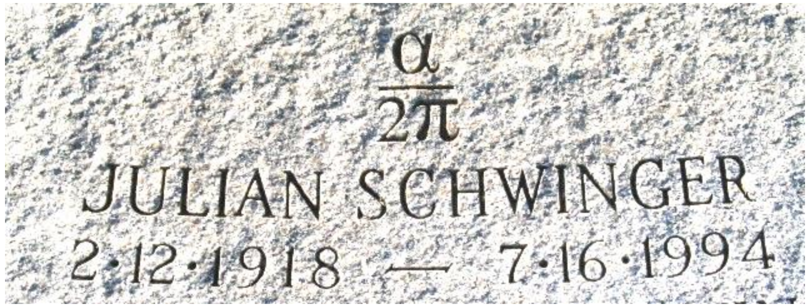

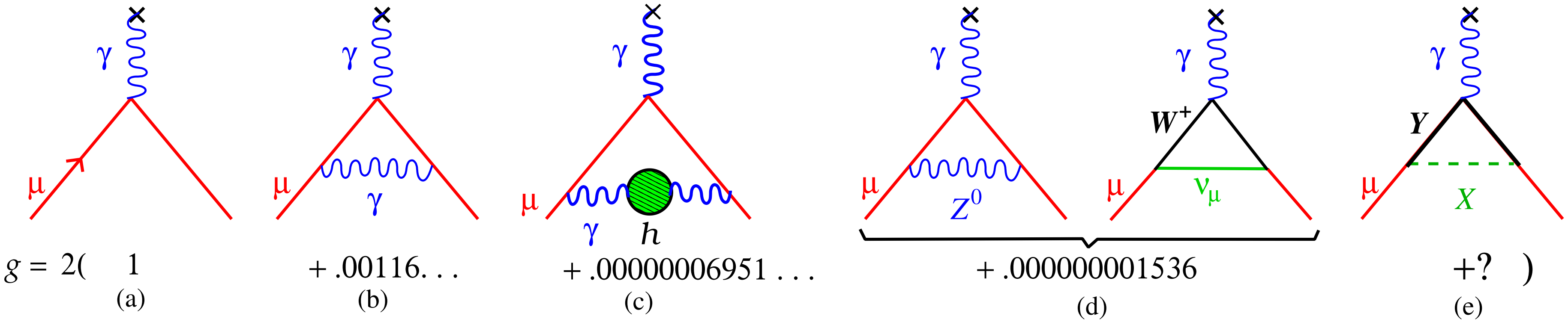

The first muon spin rotation experiment

85 MeV π^+ μ^+

degrader to stop
π^+ before C target

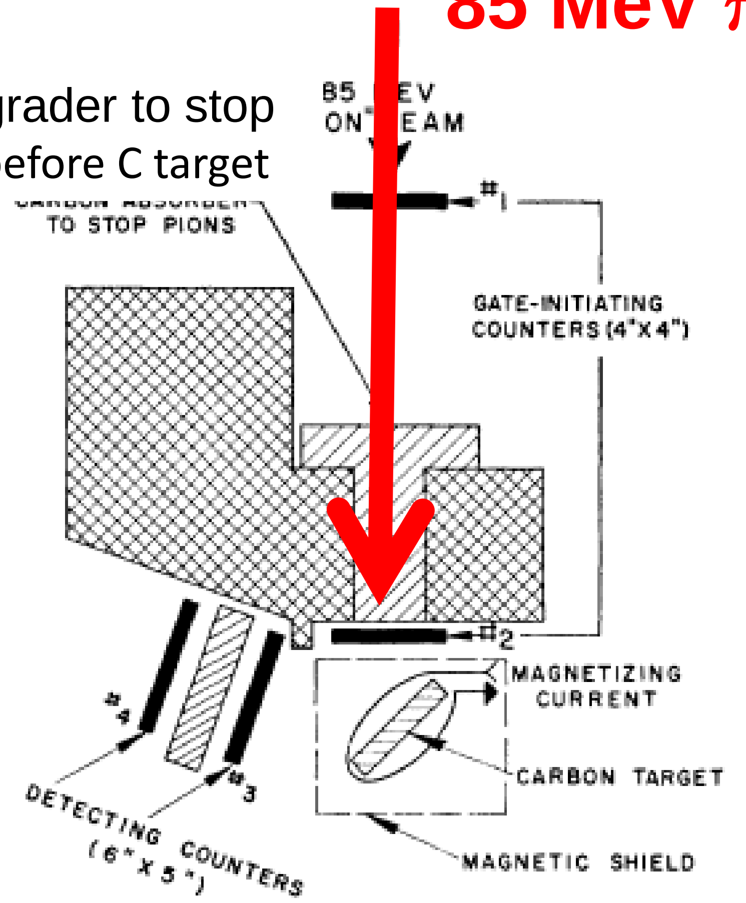

e+ detector counters

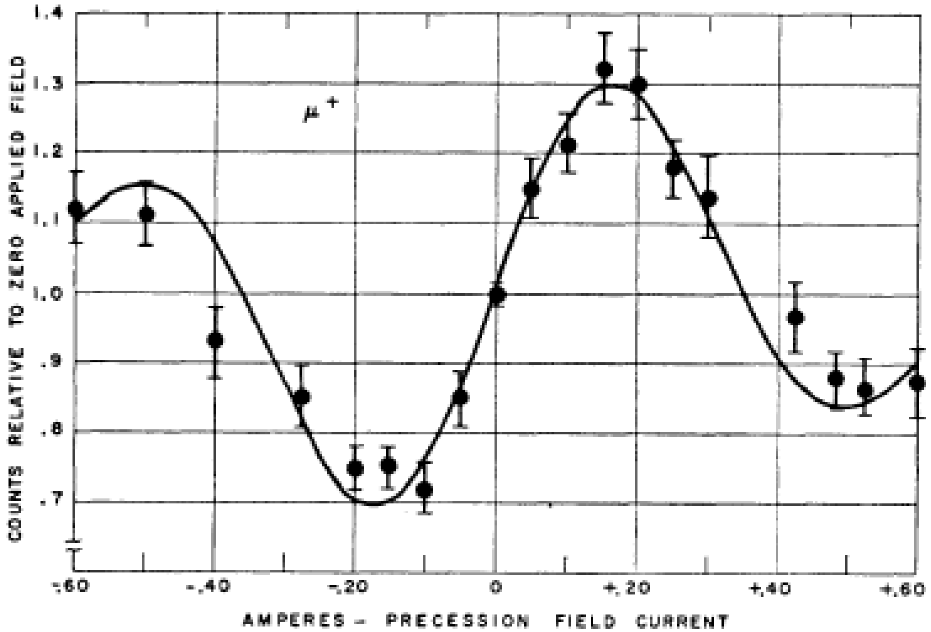

FIG. 2. Variation of gated 3–4 counting rate with magnetizing current. The solid curve is computed from an assumed electron angular distribution $1-\frac{1}{3}\cos\theta$, with counter and gate-width resolution folded in.

Fit to

$$\left(1+\frac{1}{3}\cos\theta\right)$$

Nevis Experiment

$g = 2 \pm 10\%$

R. L. Garwin, L. M. Lederman and M. Weinrich, Phys. Rev. 105, 1415 (1957), doi:10.1103/PhysRev.105.1415.

Anomalous magnetic moments (PDG)

Particle	$a_l = (g-2)/2$	SM
e	0.001 159 652 180 91 (26)	0.001 159 652 181 64 (76)
μ	0.001 165 920 89 (64)	0.001 165 918 23 (43)
τ	>-0.052 and <0.013 (95%)	0.001 177 21(5)

a_e tests QED to the precision of the fine structure constant α.

a_μ is more sensitive to heavy particle exchanges by a factor of $(m_\mu/m_e)^2$ ~42,000.

4

Muon anomaly, $a_\mu=(g-2)_\mu/2$: SM calculations and experiment

$$a_\mu^{\text{theory(SM)}} = a_\mu^{\text{QED}} + a_\mu^{\text{weak}} + a_\mu^{\text{had}}$$

$$a_\mu^{had} = \frac{\alpha^2}{3\pi^2}\int_{4m_\pi^2}^{\infty} ds\,\frac{K(s)}{s}R(s)$$

$$R(s) = \frac{\sigma(e^+e^- \to \gamma^* \to hadrons)}{\sigma(e^+e^- \to \mu^+\mu^-)}$$

QED

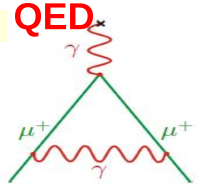

WEAK

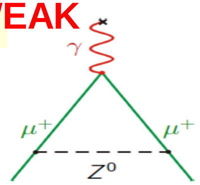

HADRONIC

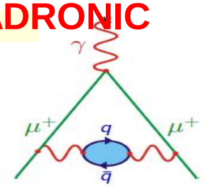

LbL

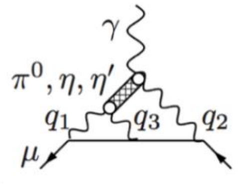

Contribution	Value $\times 10^{11}$	References
QED	116 584 718.931(104)	Refs. [33,34]
Electroweak	153.6(1.0)	Refs. [35,36]
HVP (e+e−, LO + NLO + NNLO)	6845(40)	Refs. [2–8]
HLbL (pheno + lattice + NLO)	92(18)	Refs. [18–32]
Total SM Value Section	116 591 810(43)	Refs. [2–8,18–24,31–36]
Exp. (E821) - SM	279(76)	

The table is from:
"The anomalous magnetic moment of the muon in the Standard Model", T. Aoyama et al., Physics Reports 887 (2020) 1–166

n

SM calculations and experiment

Since new experiments at FNAL and JPARC expect to improve the accuracy of muon (g-2) by factor 3, we need in a precision of the hadronic cross section at the level of 0.3%

$a_\mu^{had,LO\text{-}VP}$

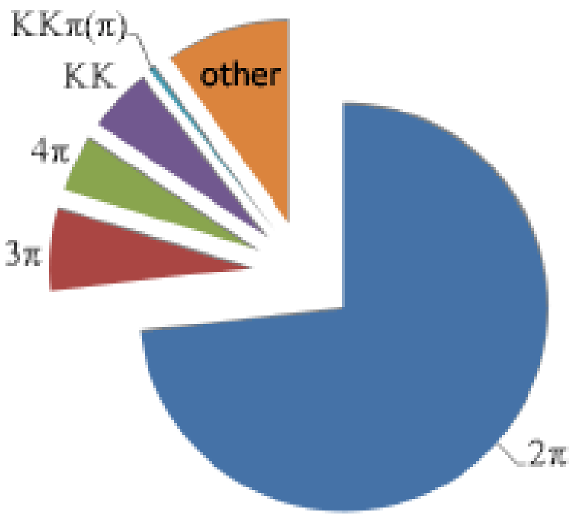

$a_\mu^{had,LO\text{-}VP}$ error squared

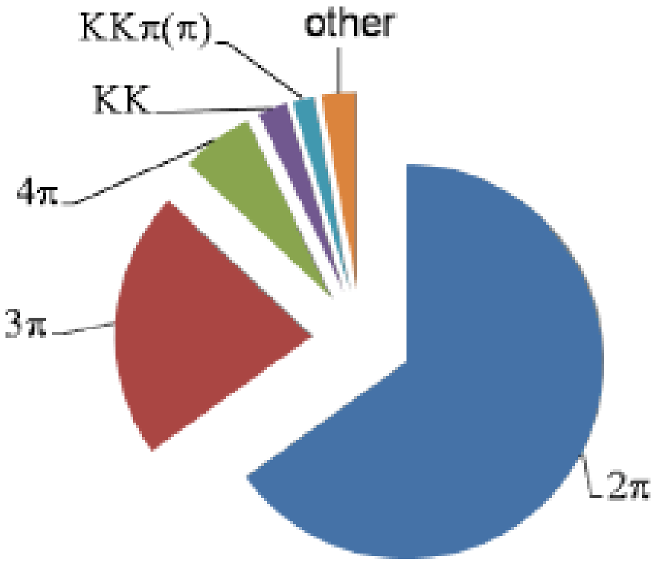

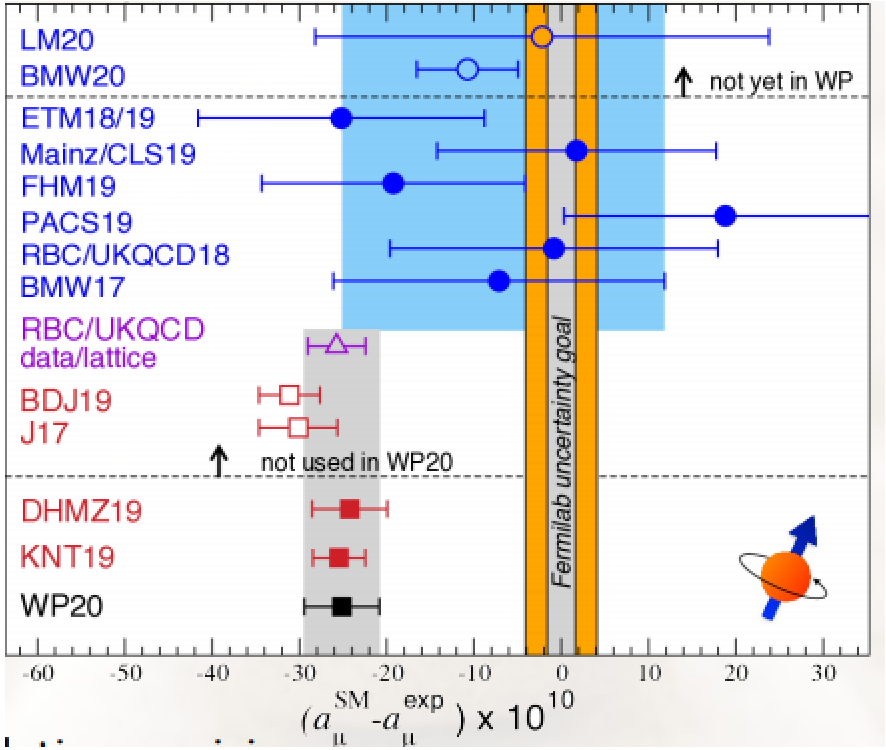

e-Print: 2203.15810

1 September 1967

INVESTIGATION OF THE ρ-MESON RESONANCE WITH ELECTRON-POSITRON COLLIDING BEAMS

V. L. AUSLANDER, G. I. BUDKER, Ju. N. PESTOV, V. A. SIDOROV, A. N. SKRINSKY and A. G. KHABAKHPASHEV
Institute of Nuclear Physics, Siberian Branch of the USSR Academy of Sciences, Novosibirsk, USSR

Received 1 September 1967

Preliminary results on the determination of the position and shape of the ρ-meson resonance with electron-positron colliding beams are presented.

When experiments with electron-positron colliding beams were planned [1,2] investigation of the process

$$e^- + e^+ \to \pi^- + \pi^+$$
$$e^- + e^+ \to K^- + K^+$$

Start of e+e- → hadrons measurements

Phys.Lett. 25B (1967) no.6, 433-435

VEPP-2, Novosibirsk

Detector was made from different layers of Spark chambers,
readouts by photo camera

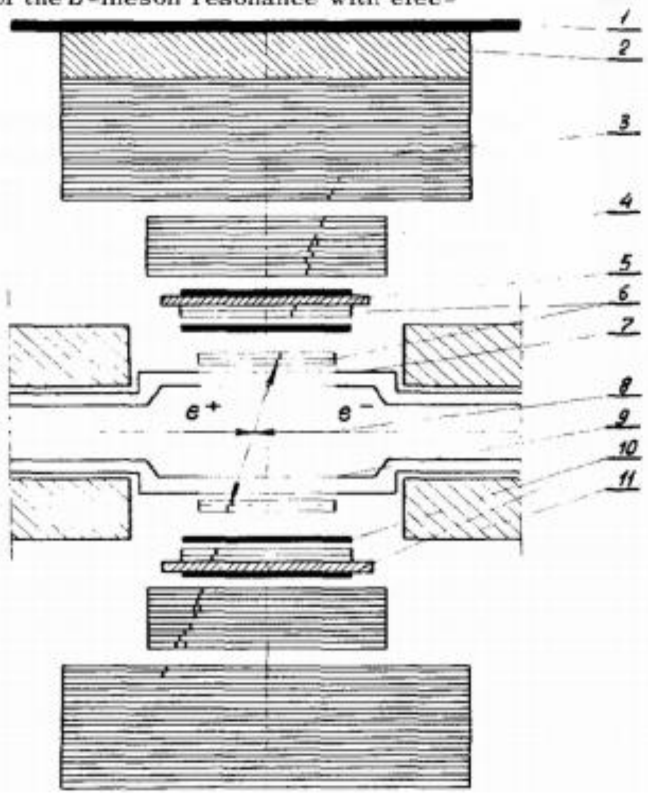

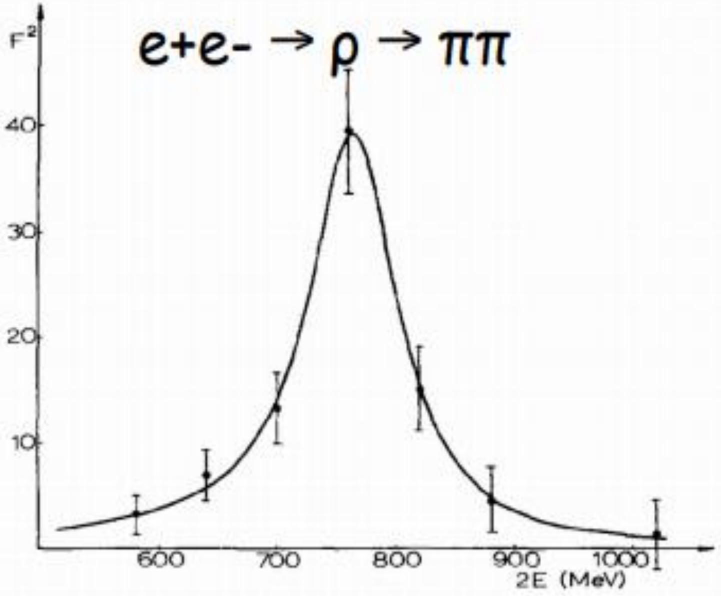

Fig. 2. Experimental values of $F^2(E)$ approximated by the Breit-Wigner formula.

1985 - VEPP-2M with more detailed scan OLYA systematic 4%, CMD 2%

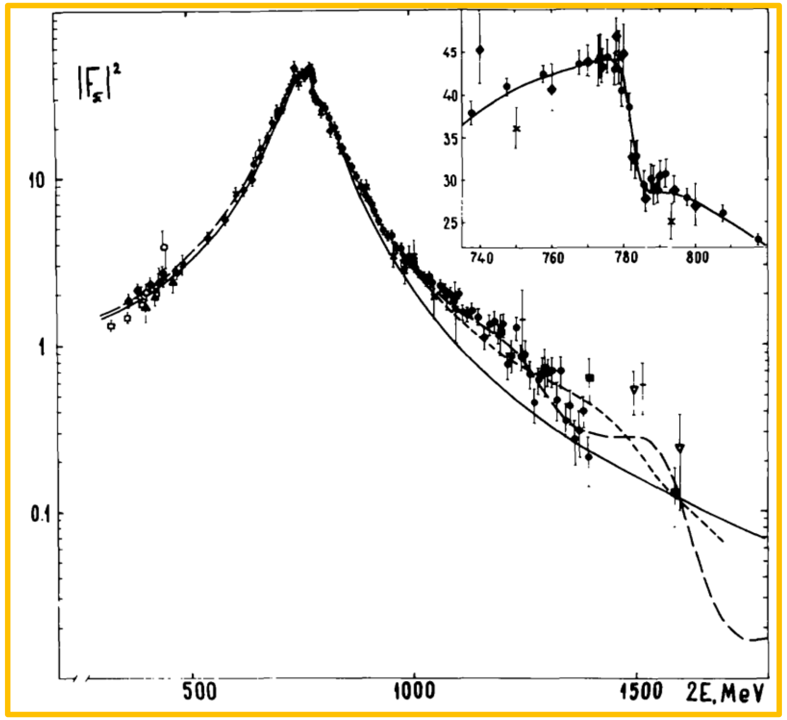

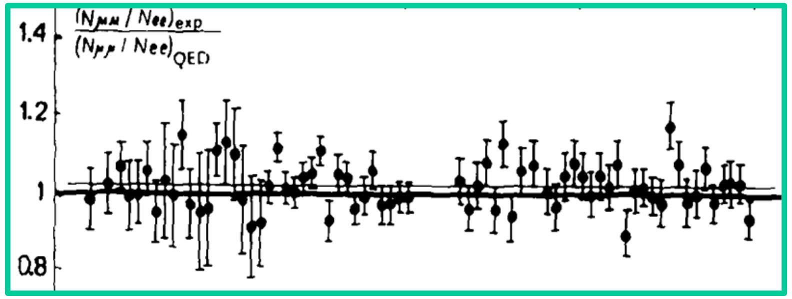

Due to preparation of the E821 experiment at BNL Prof. Vernon Hughes came to BINP in the end of eighties to convince people to measure $R_{had} = \sigma_{had}/\sigma_{\mu\mu}$ with 1% accuracy. That time this looks to be almost impossible.

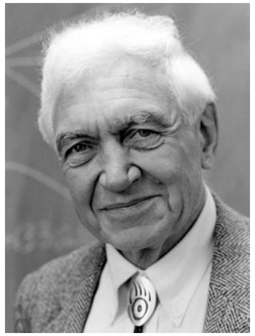

2004 with CMD2 at VEPP-2M

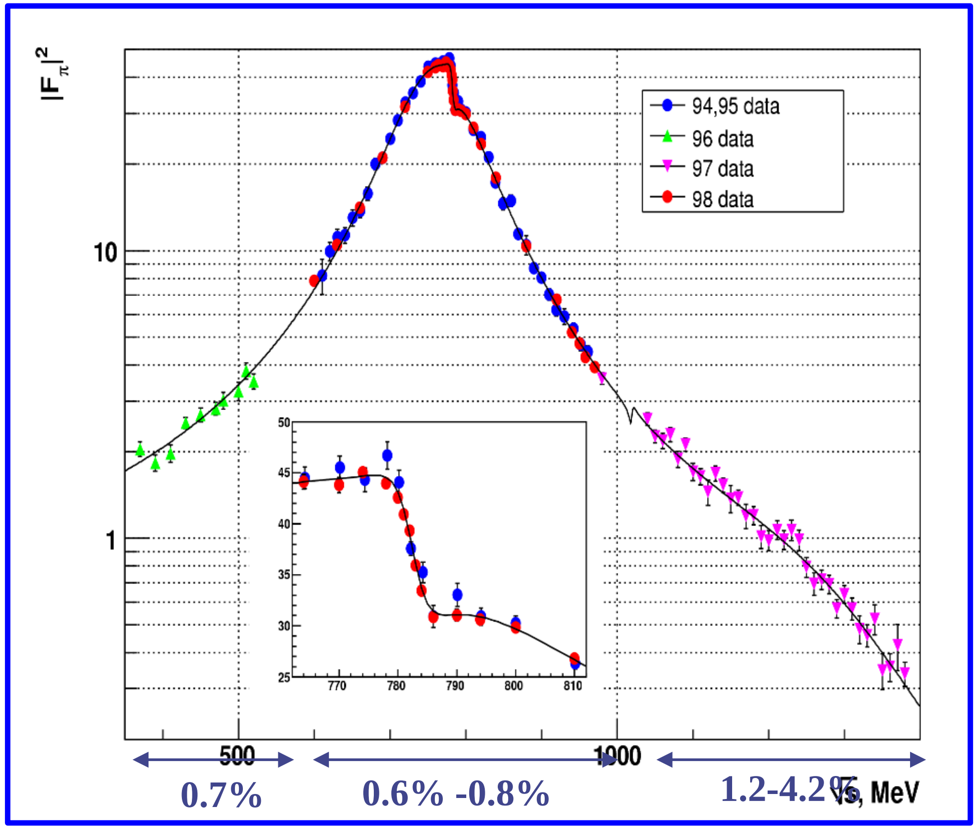

Systematic error

It took almost 20 years to achieve this accuracy.

R measurement – exclusive vs inclusive

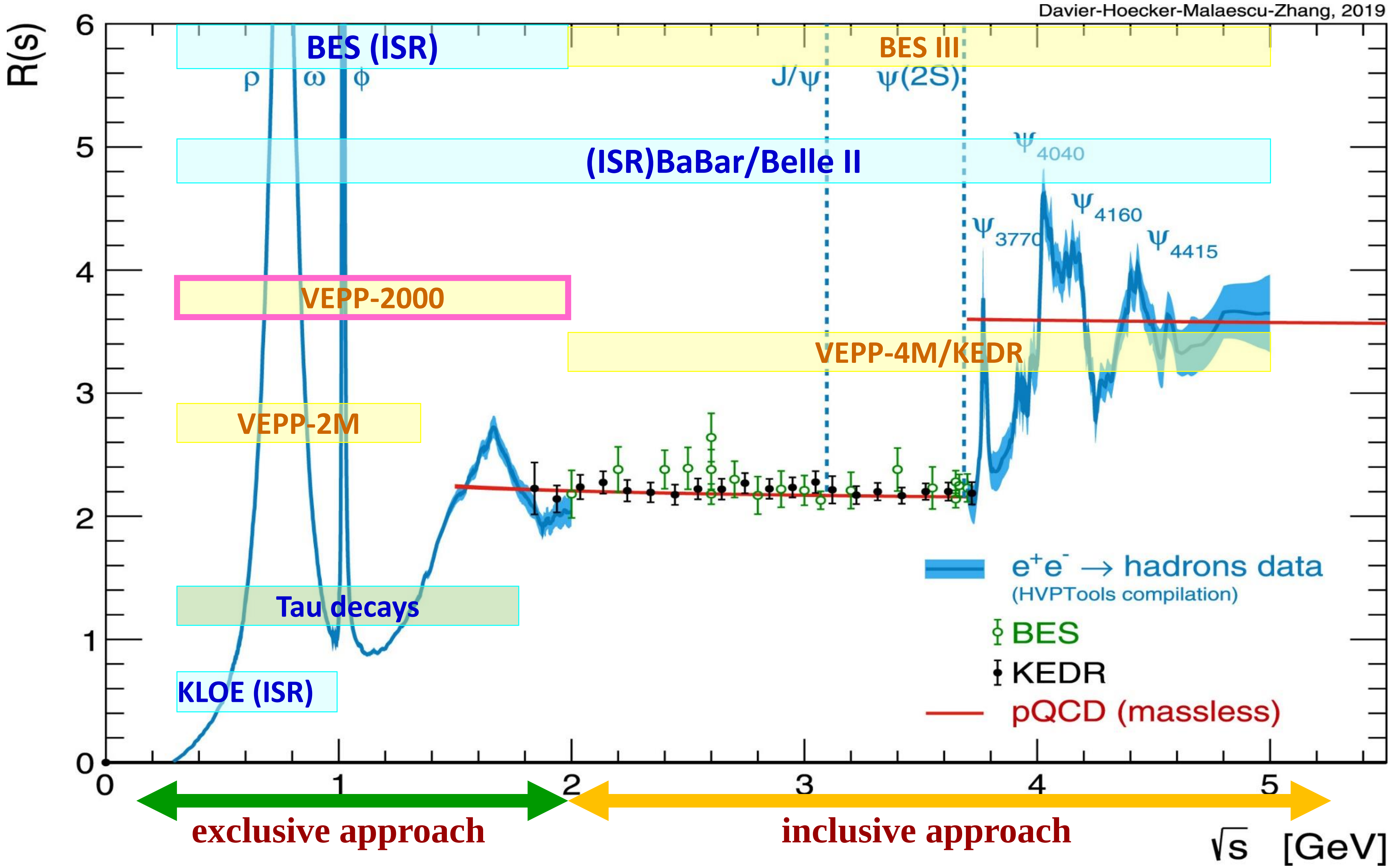

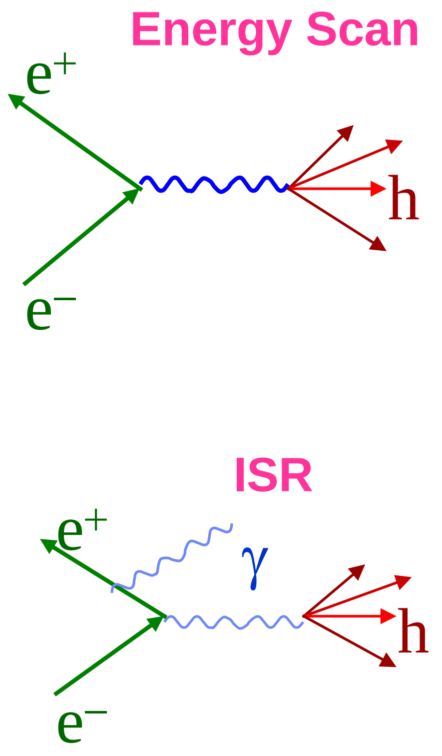

The figure is from:
"The anomalous magnetic moment of the muon in the Standard Model", T. Aoyama et al., Physics Reports 887 (2020) 1–166.

VEPP-2000 after upgrade (from 2017)

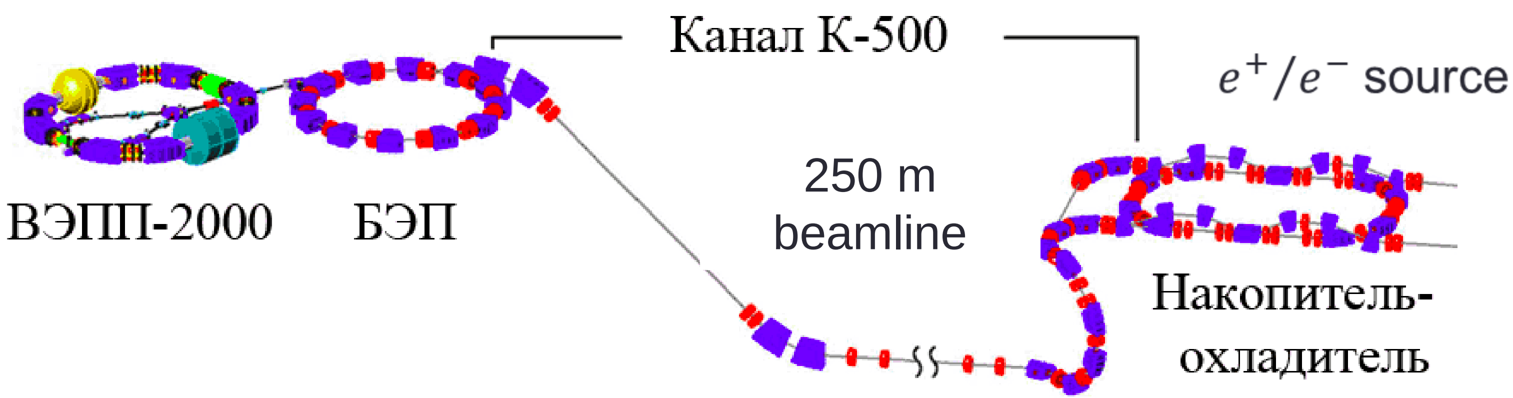

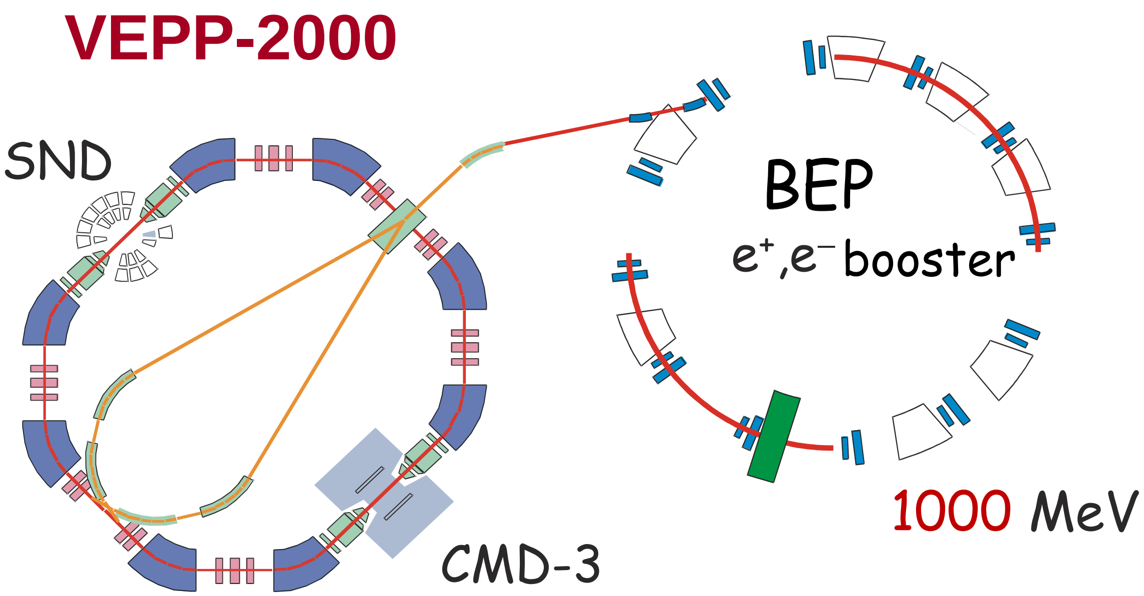

The main idea – round beams!

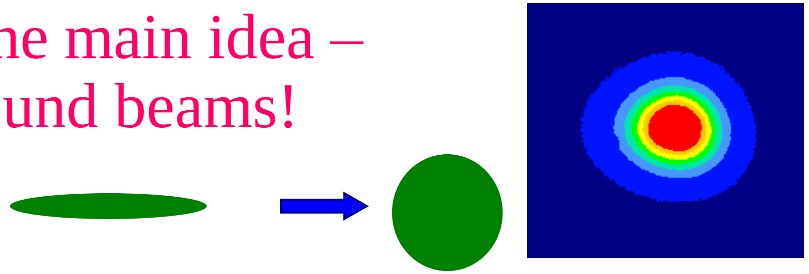

VEPP-2M & VEPP-2000 parameters

	VEPP-2M	VEPP-2000	
E (MeV)	510	510	900
Π (cm)	1788	2235	2235
$\mathcal{I}^+, \mathcal{I}^-$ (mA)	40	34	200
$\varepsilon \cdot 10^5$ (cm · rad)	3	0.5	1.6
β_x (cm) β_z (cm)	40 5	6.3 6.3	6.3 6.3
ξ_x ξ_z	0.016 0.050	0.075 0.075	0.075 0.075
$\mathcal{L}(\mathrm{cm^{-2}s^{-1}})$	$3 \cdot 10^{30}$	$1 \cdot 10^{31}$	$1 \cdot 10^{32}$

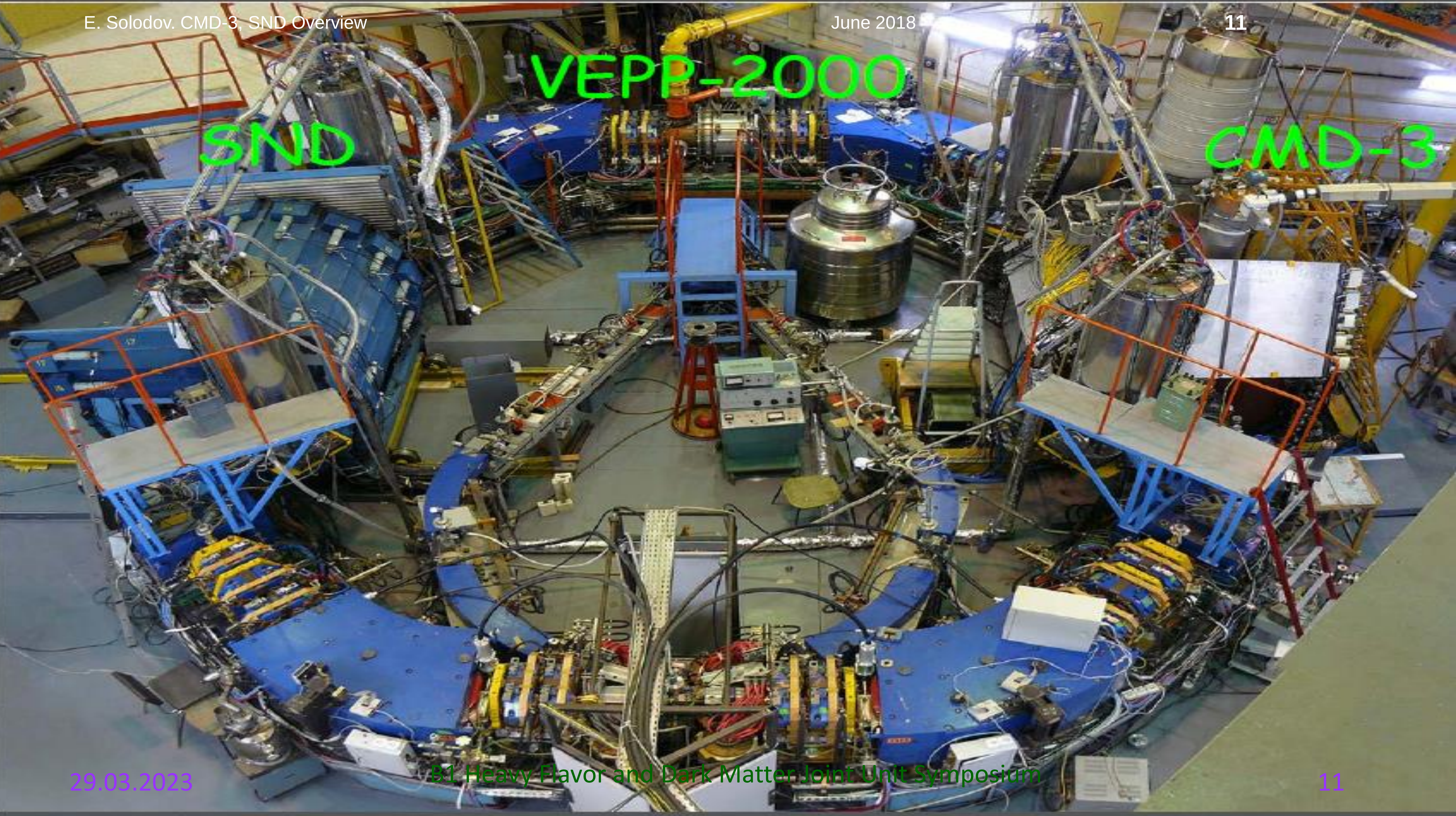
VEPP-2000
SND
CMD-3

Energy measurement

Starting from 2012, energy is monitored continuously using compton backscattering techneques

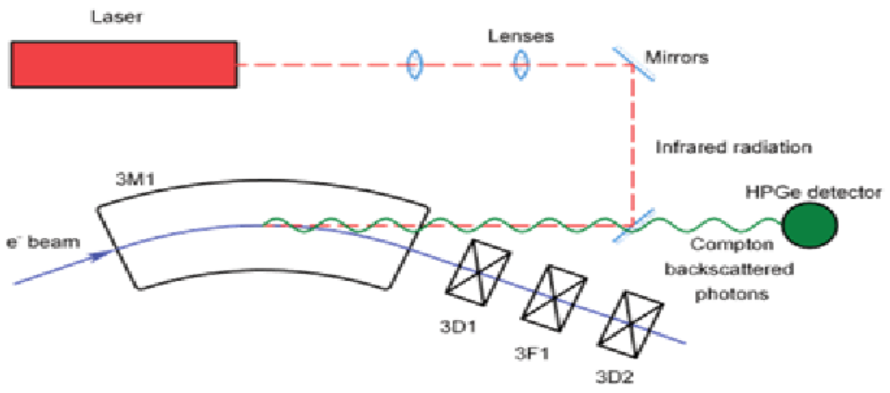

Radiation coming from A and C points under angle φ = 0 is interferenced

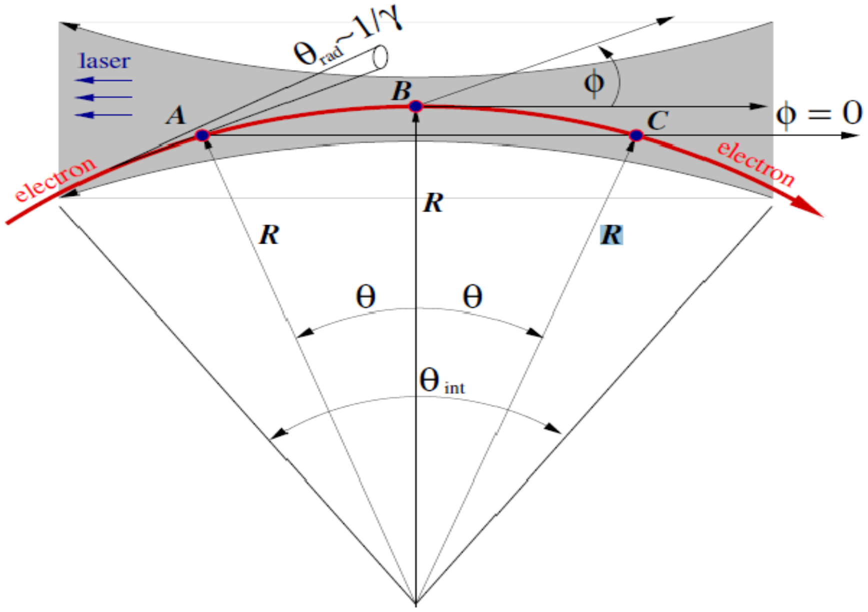

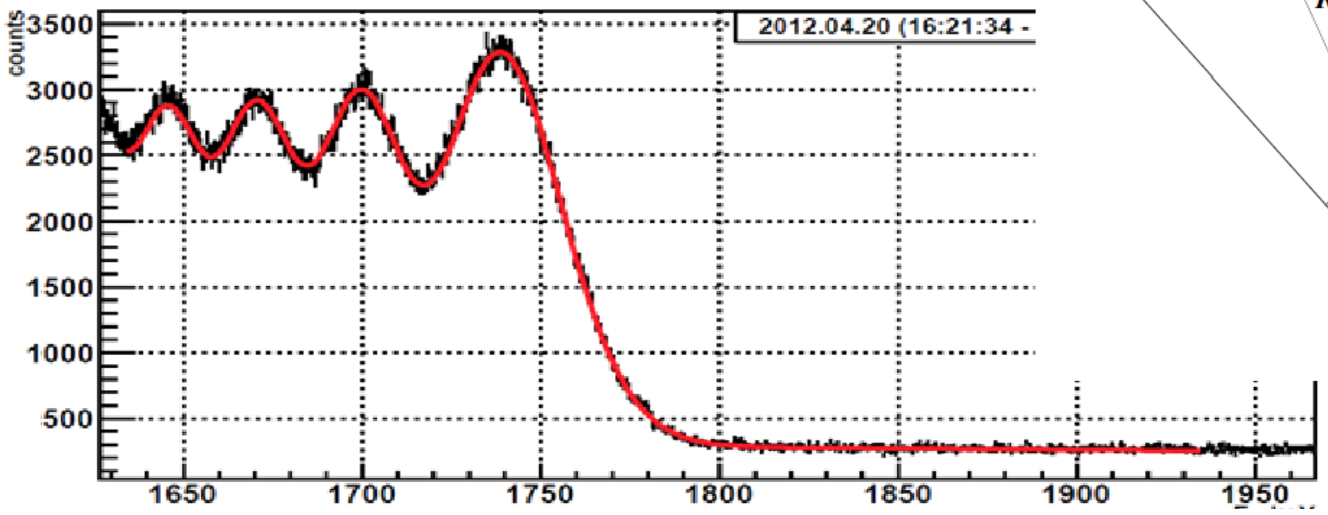

E = 993.662 ± 0.016 MэB

E.V. Abakumova et al., Phys. Rev. Lett. 110 (2013) 14, 140402,
E.V. Abakumova et al.,Nucl.Instrum.Meth. A744 (2014) 35-40

CMD-3 - detector

Compact multipurpose detector comprising magnetic spectrometry with high resolution calorimetry

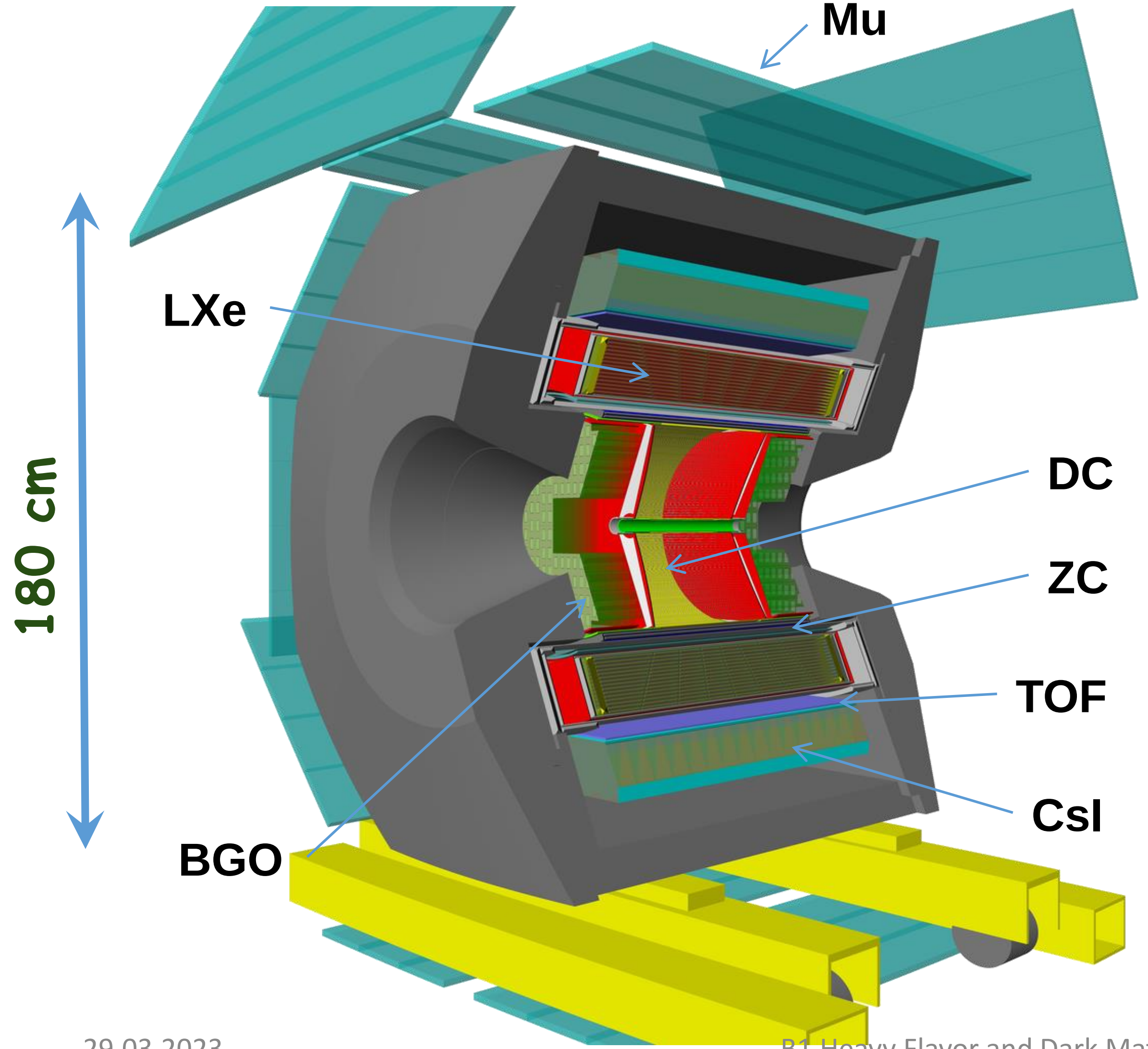

Magnetic field: 1.3T

Track reconstruction:

$\sigma_{\rho\varphi} \approx 100$ µm,

$\sigma_z \sim 2 - 3$ mm

$\sigma_p/p \approx \sqrt{(4.4p[GeV])^2 + 0.62\%}$

Combined EM-calorimeter:

Barrel: 5.3 X_0 LXe + 8.1X_0 CsI = 13.5 X_0

$\sigma_E/E \approx (3.4/\sqrt{E[GeV]} \oplus 2)\%$

$\sigma_\omega \approx$ 5 mrad

End caps: BGO (14.4 X_0)

TOF: $\sigma_t \approx$ 1 ns

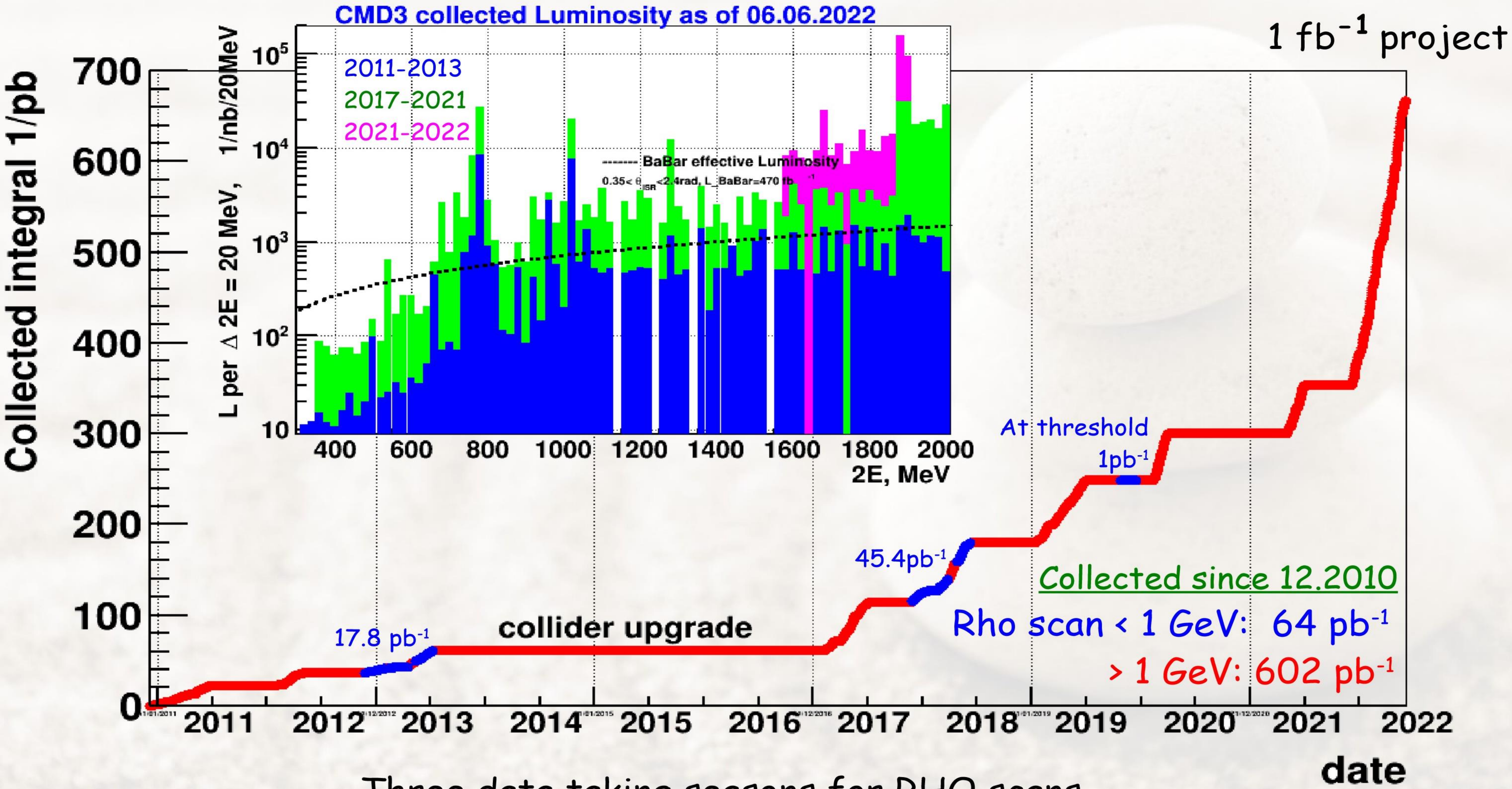

Three data taking seasons for RHO scans

CMD-3 results and analyses ongoing

Published

$3(\pi^+\pi^-)$	PLB 723 (2013) 82
$e^+e^- \to \eta'(958)$	PLB 740 (2015) 273
$p\bar{p}$	PLB 759 (2016) 634
$K^+K^-\pi^+\pi^-$	PLB 756 (2016) 153
K_SK_L	PLB 760 (2016) 314
K^+K^-	PLB 779 (2018) 64
$\pi^+\pi^-\ \pi^+\pi^-$	PLB 768 (2017) 345
$\omega\eta$, $\pi^+\pi^-\ \pi^0\eta$	PLB 773 (2017) 150
$3(\pi^+\pi^-)\pi^0$	PLB 792 (2019) 419
$K^+K^-\eta$	PLB 798 (2019) 134946
$\eta\pi^+\pi^-$	Journal of HEP, 2020, 2020(1), 112

Analyses ongoing

$e^+e^- \to \pi^+\pi^-$

$\pi^+\pi^-\ \omega$

$e^+e^- \to$ D0*

$K_SK^+\pi^-$

$2(\pi^+\pi^-)\pi^0$, $2(\pi^+\pi^-\ \pi^0)$

$\pi^+\pi^-\ \eta(3\pi, 2\gamma)$

$K^+K^-\ \omega$, $K^+K^-\ \eta$

$K^+K^-\ \pi^0$, $K_SK_L\pi^0$, $K_SK_L\eta$

K^+K^-, K_SK_L

$\pi^+\pi^-\pi^0\pi^0$, $2(\pi^+\pi^-)$

$n\bar{n}$

$\eta\gamma$, $\pi^0\gamma$,

$\omega \to \pi^0\ e^+e^-$, ηe+e-

CMD-3 data samples

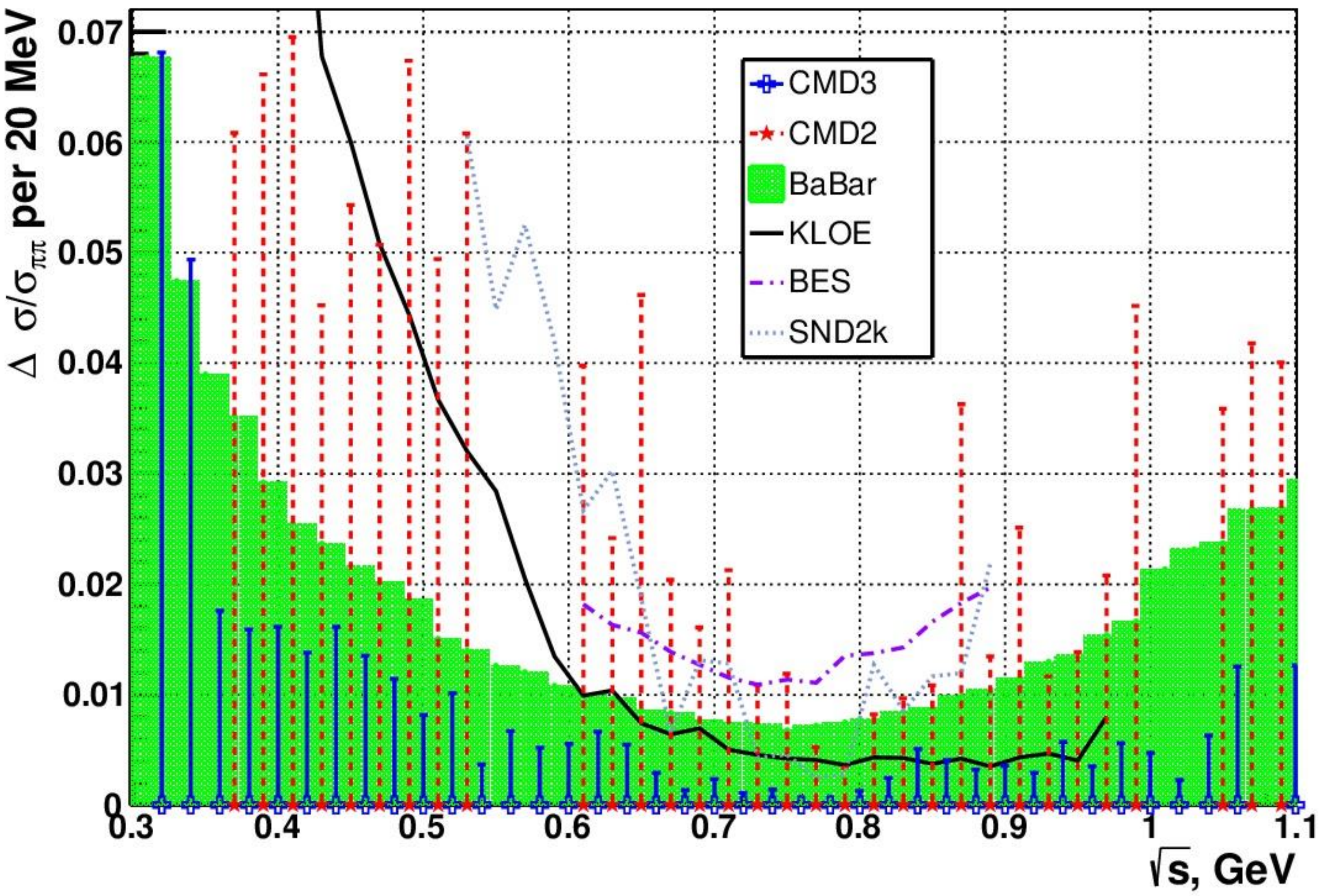

Events under study are very simple with only 2 collinear tracks. However, the required extremely high precision (target systematics 0.35-0.5%) makes this measurement very challenging!

Analysis based on L = 61.9 pb^{-1} at $\sqrt{s}$ < 1 GeV:
RHO2013
RHO2018
LOW2020
and 25.7 pb^{-1} @ 1.0-1.2 GeV

$34\times10^6\ \pi^+\pi^-$, $3.7\times10^6\ \mu^+\mu^-$, 44×10^6 e^+e^- events selected at $\sqrt{s}$ < 1 GeV

Pion Form Factor evaluation

$$\sigma_{e^+e^-\to\pi^+\pi^-} = \sigma^0_{\pi^+\pi^-}|F_\pi|^2 = \frac{\pi\alpha^2}{3s}\beta_\pi^3|F_\pi|^2$$

Main issues for this analysis:
- **e/μ/π separation**
- **radiative corrections**
- **precise fiducial volume**

The main idea is to minimize simulation usage, to rely mostly on data

$$|F_\pi|^2 = \left(\frac{N_{\pi^+\pi^-}}{N_{e^+e^-}} - \Delta^{bg}\right)\frac{\sigma^0_{e^+e^-}(1+\delta^{rad}_{e^+e^-})}{\sigma^0_{\pi^+\pi^-}(1+\delta^{rad}_{\pi^+\pi^-})}\frac{\epsilon_{e^+e^-}}{\epsilon_{\pi^+\pi^-}}$$

Ratio Nππ/Nee is measured
directly, the detector inefficiencies are partially cancelled out

Background is low

Radiative corrections defined in used acceptance, account for ISR and FSR effects, VP included in Fπ definition.

Efficiency analysis rely mostly on the data. Important only difference between π+π- / e+e-
(common cancelled out)

Event selection

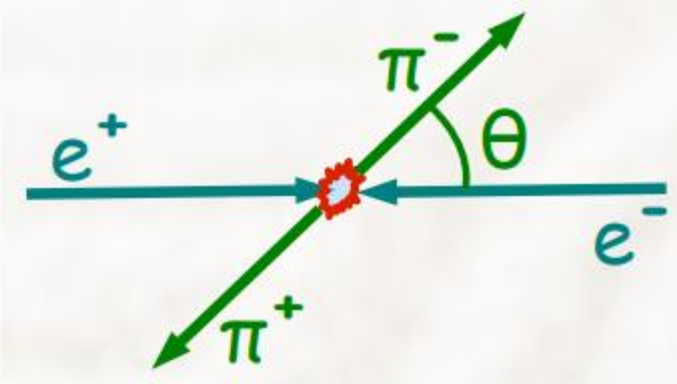

Simple event signature with
2 back-to-back charged particles

- Two charged collinear tracks:
  |Δφ|<0.15, |Δθ|<0.25, Q1+Q2=0,|Δ t|<20 nsec
- Vertex position close to interaction point:
  Ro average <0.3см, |Z average|<5см
  |Δρ|<0.3см, |ΔZ|<5см
- Fiducial volume inside good region of the DCH:
  1.<(π+θ+−θ−)/2<π−1. rad
- Quality of selected tracks:
  χ2/ndf<10,Nhit≥10
- Filtration of low momentum and cosmic background:
  0.45Ebeam <p±<Ebeam+100MeV/c, p±>1.15pK±

Data sample includes events with: e+e-, μ+μ-, π+π-, cosm
Almost no other background at √s <1 GeV

$34\times10^6\ \pi^+\pi^-$, $3.7\times10^6\ \mu^+\mu^-$, 44×10^6
e^+e^- events selected at $\sqrt{s} < 1$ GeV

Event separation

Two main methods
1) by momentum
2) or by energy deposition
Two additional for cross-check
3) by angular distribution
4) using shower profile at >1GeV

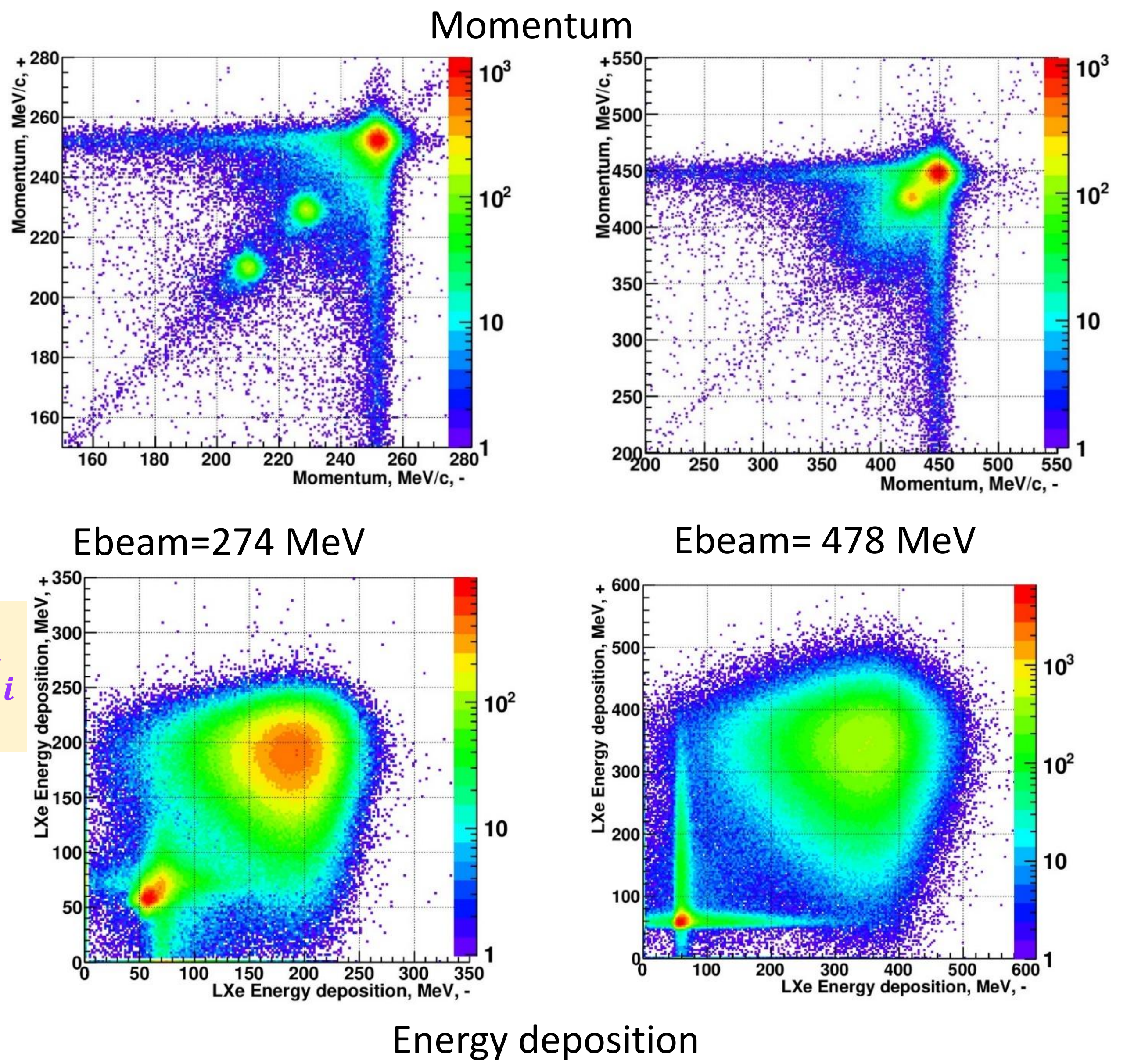

To obtain the number of events of each process the likelihood function was used

$$-\ln L = -\sum_{events} \ln\left[\sum_i N_i f_i\,(X^+, X^-)\right] + \sum_i N_i$$

Momentum-based separation:
PDFs are constructed as: MC generator spectra are convolved with detector response function (momentum resolution, bremsstrahlung, pion decays) 36 free parameters in fit per each point

Energy deposition-base separation:
PDFs is described by a generic functional form (log-gaus, etc), trained on the data: by tagged electron, cosmic muons, 57 free parameters in fit

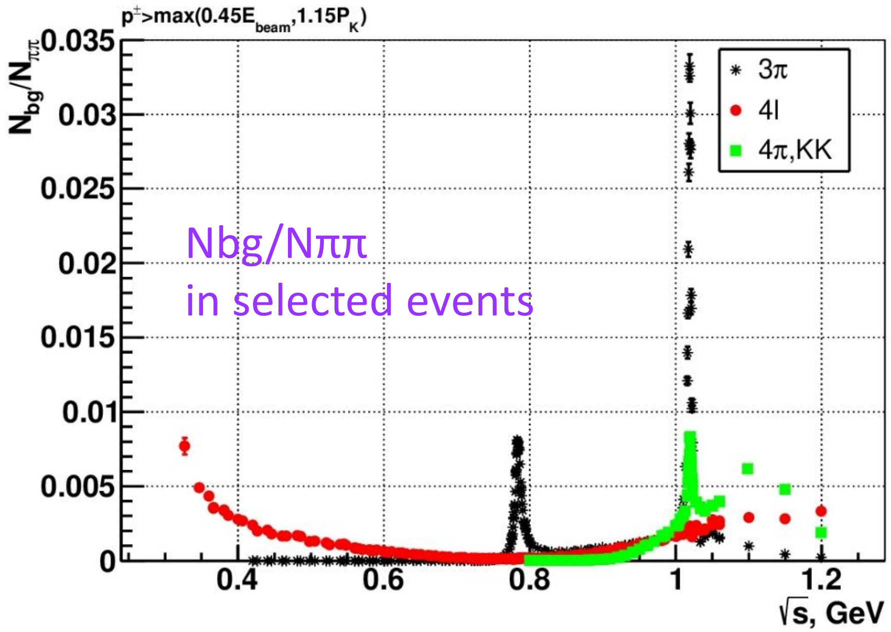

Contribution of background processes to collinear events:

$e^+e^- \to \pi^+\pi^-\pi^0$; $e^+e^- \to e^+e^-e^+e^-$, $e^+e^-\mu^+\mu^-$;

$e^+e^- \to K^+K^-$, K_SK_L, $\pi^+\pi^-\pi^+\pi^-$, $\pi^+\pi^-\pi^0\pi^0$

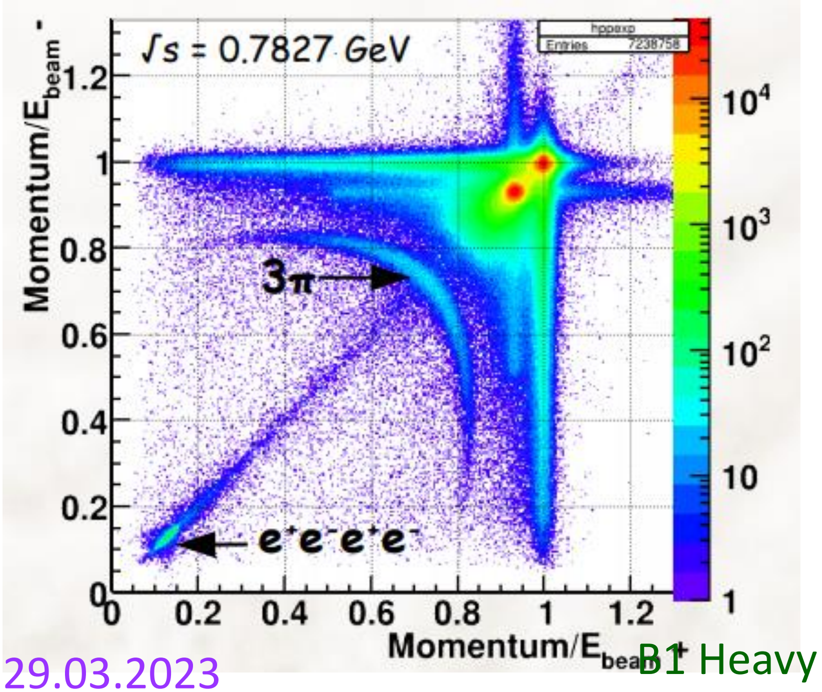

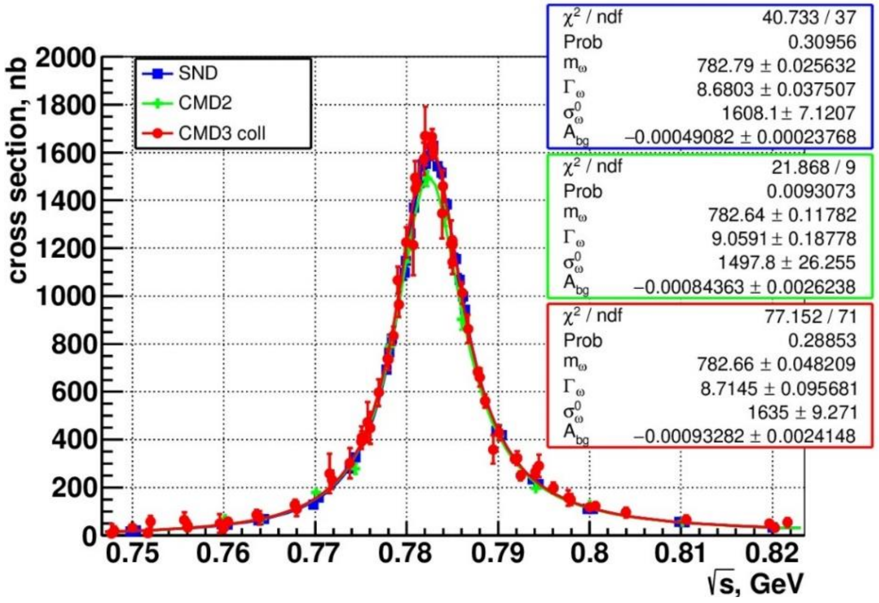

$B(\omega \to e^+e^-)B(\omega \to \pi^+\pi^-\pi^0) = (6.82 \pm 0.04 \pm 0.23)\times 10^{-5}$

Detection efficiency

Assuming independence of the calorimeter & tracker (DC), the track reconstruction inefficiency were estimated using the “test” sample with based two collinear clusters in the LXe and one good track in DC

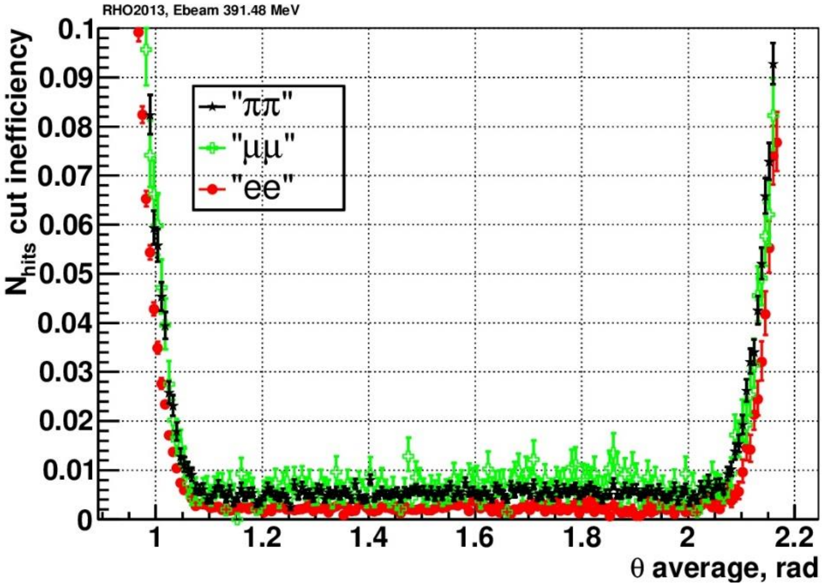

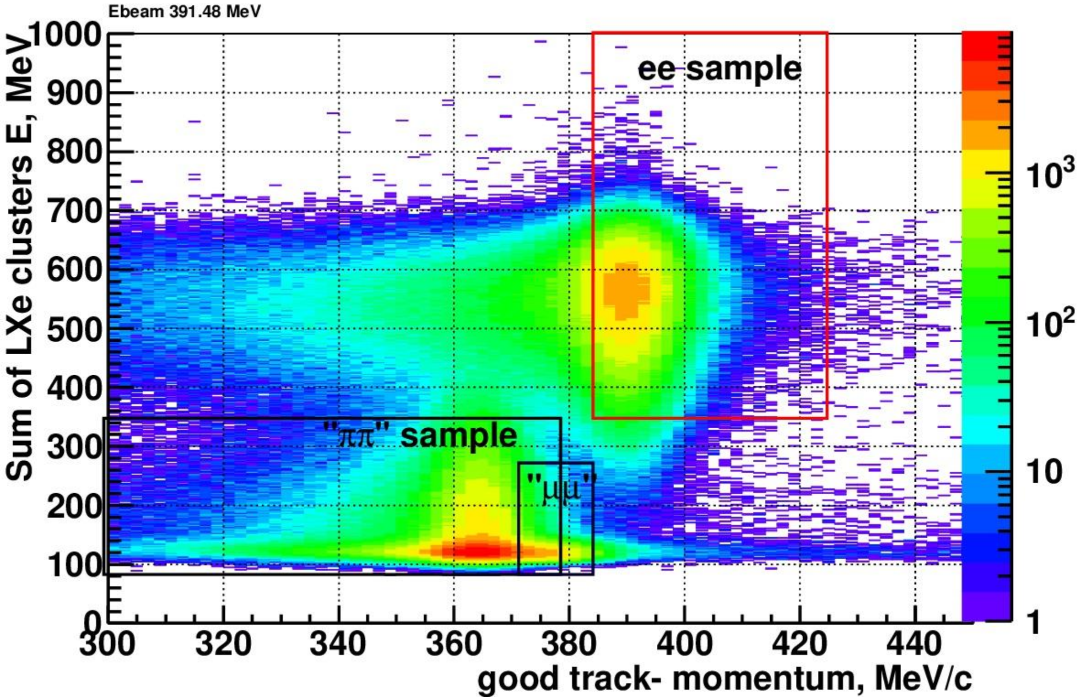

Efficiency without particles specific losses

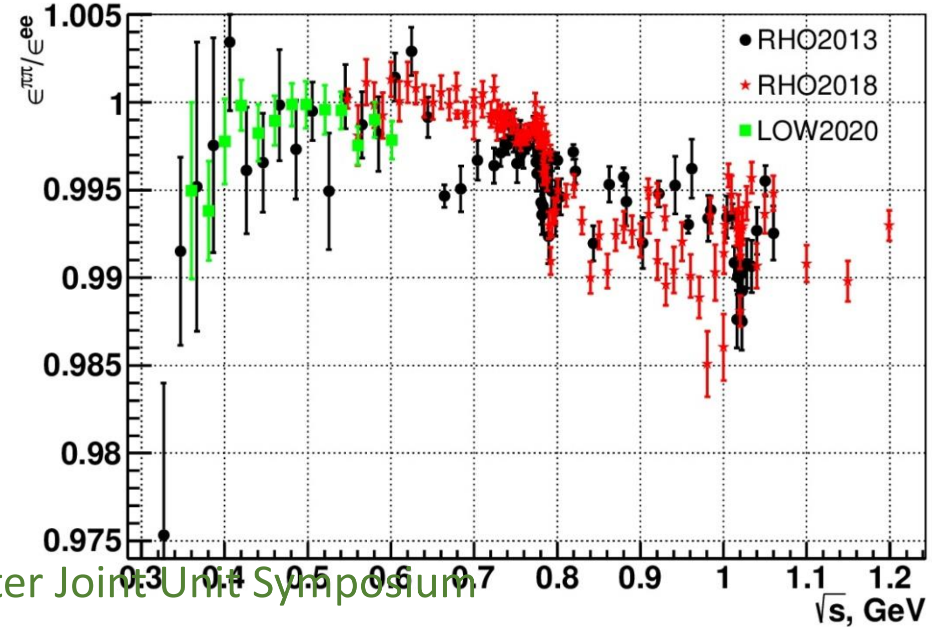

Particle specific losses

Bremsstrahlung energy loss, decay in flight, nuclear interaction with materials, MS on the inner vacuum tube, etc

Taken from detailed full MC (including detector conditions with time)

but is also controlled by the data

nuclear interactions mostly on inner tube (systematics 0.2%)

most dangerous is decay in flight as it depends on detector conditions (syst. 0.2-0.1%)

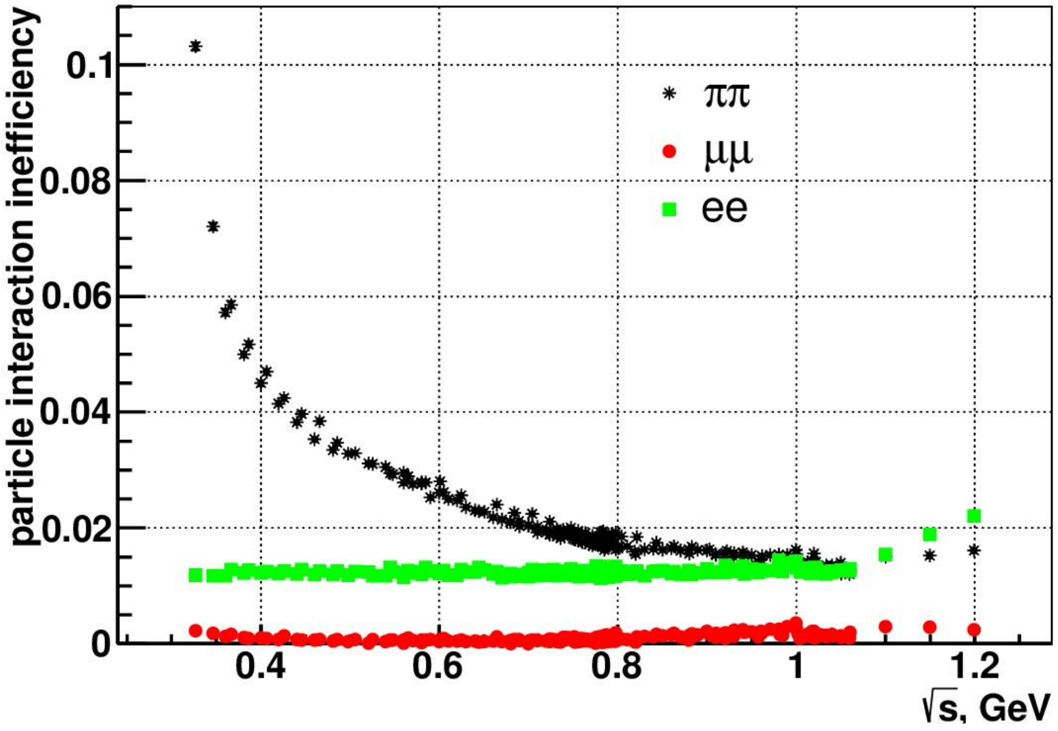

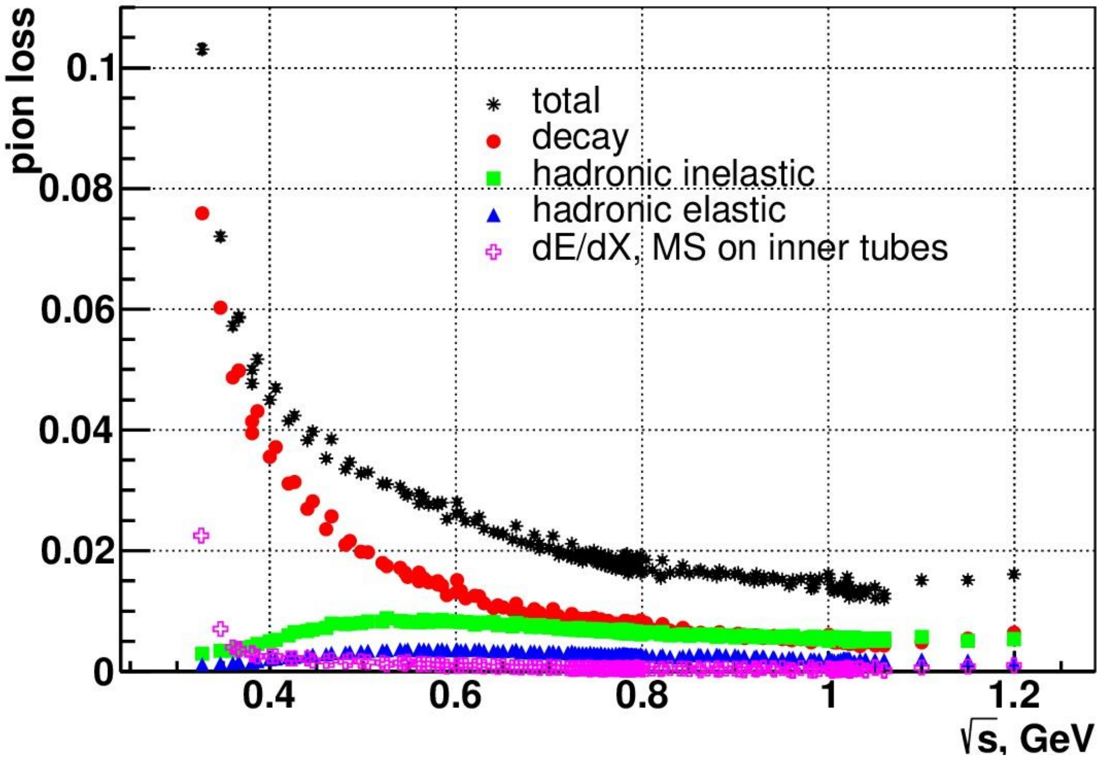

Trigger efficiency

Having two "independent" triggers allows to study an efficiency of certain one by requiring that other presents in an event:

Trigger efficiencies are evaluated from dependence with polar angle (TF), with energy of two clusters (CF)

Total TF|CF: → ~ >0.9994 for 2π events (and higher for e+e-)

Efficiency correction accounts for correlation via time response

Out-of-sync trigger issue gives 0.1-0.5% effect to lose both tracks

→ trigger systematics **0.05% (<1GeV) – 0.3% (>1GeV)** – as difference between 2π/e+e

$$\epsilon_{TF}^{trig} = (N_{TF\&CF} / N_{CF}) / (\epsilon_{TF\&CF}^{rec} / \epsilon_{CF}^{rec})$$

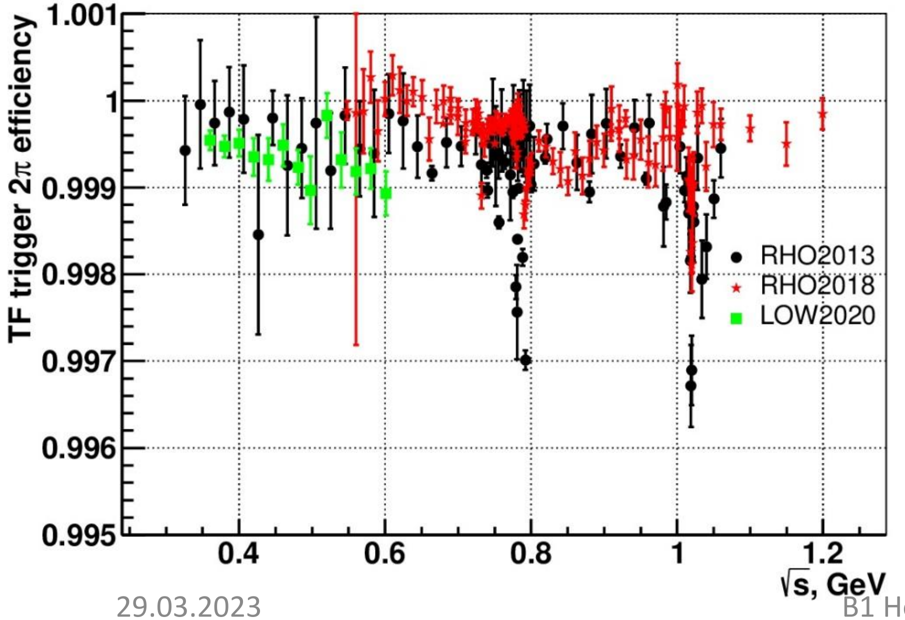

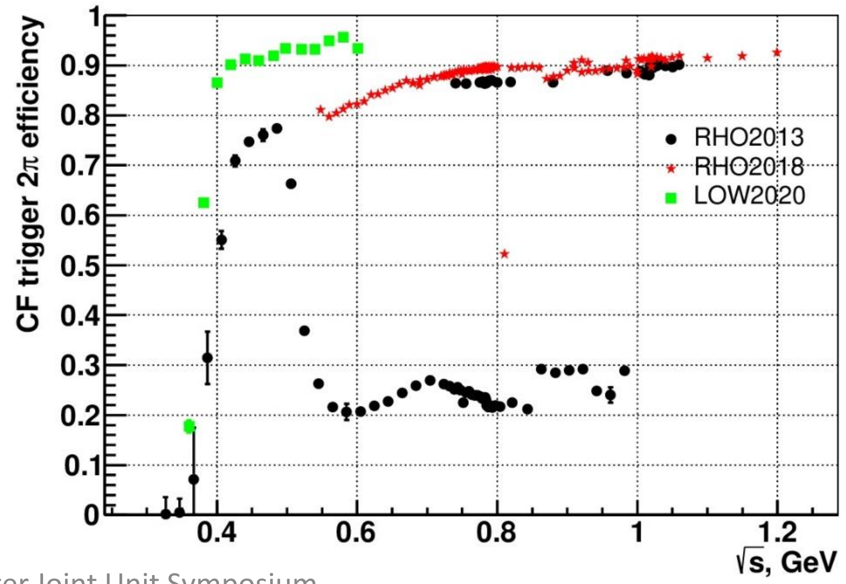

Total efficiency

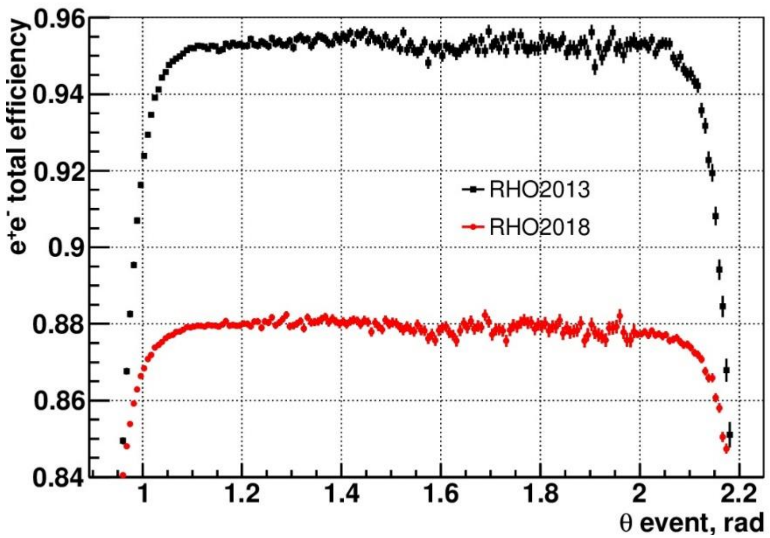

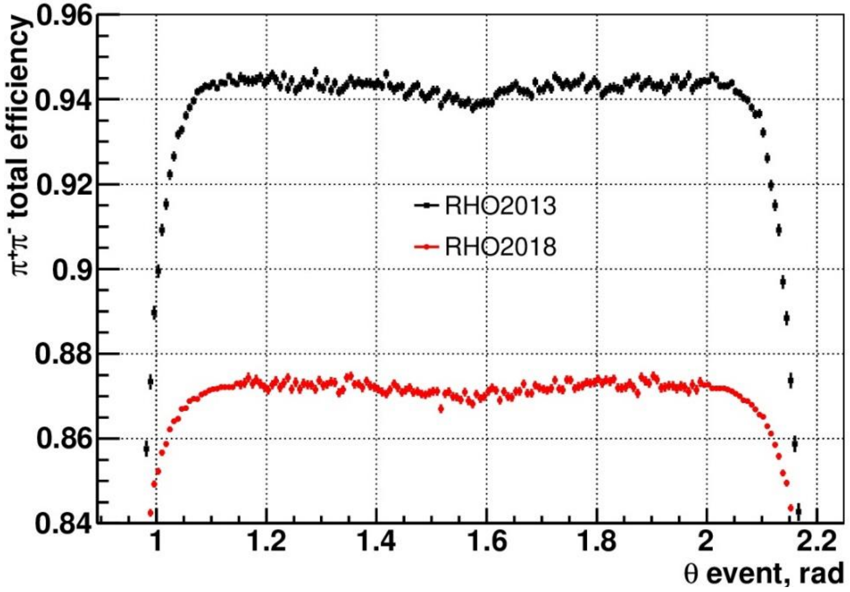

includes all the known effects. The main efficiency loss comes from the Z vertex selection with the average 97.0% and 89.2% for the RHO2013 and RHO2018 data respectively and it is near same for $\pi+\pi-$ and $e+e-$ events. The efficiency dependence is well symmetric over $\theta = \pi/2$ radian, with small dependence at the level $0.2 \div 0.3\%$ for $e+e-$ events because of not symmetric differential cross section. The decreasing of the efficiency at level $\Delta \sim 0.4 - 0.5\%$ for $\theta \sim \pi/2$ radians comes from the Z vertex selection and the polar angle resolution effects. The angle resolution changes by factor of 2 from $\theta = 1$ to $\pi/2$ radians due to the charge screening effect, reducing amplitudes for the perpendicular to the wires tracks in the DCH. The drop of the efficiency by 2% and 4.5% at the edge of the used angles range comes from the requirement on the number of hits in the DCH.

Radiative corrections

To achieve ultimate precision in $e^+e^- \to \pi^+\pi^-$ measurements we have know the radiative corrections wery accurately.

Two high precision MC generators are used:
MCGPJ (0.2%, e^+e^-, $\mu^+\mu^-$, $\pi^+\pi^-$) and
BabaYaga@NLO (0.1%, e^+e^-, $\mu^+\mu^-$)

In this study the radiation corrections should be taken into account for total cross section determination but these are important as well for differential momentum distribution used in the momentum-based separation.

After detail studies we adopted this generators usage:
e^+e^- : BabaYaga@NLO
$\mu^+\mu^-$: BabaYaga@NLO (differential cross section)
MCGPJ (integral)
$\pi^+\pi^-$: MCGPJ

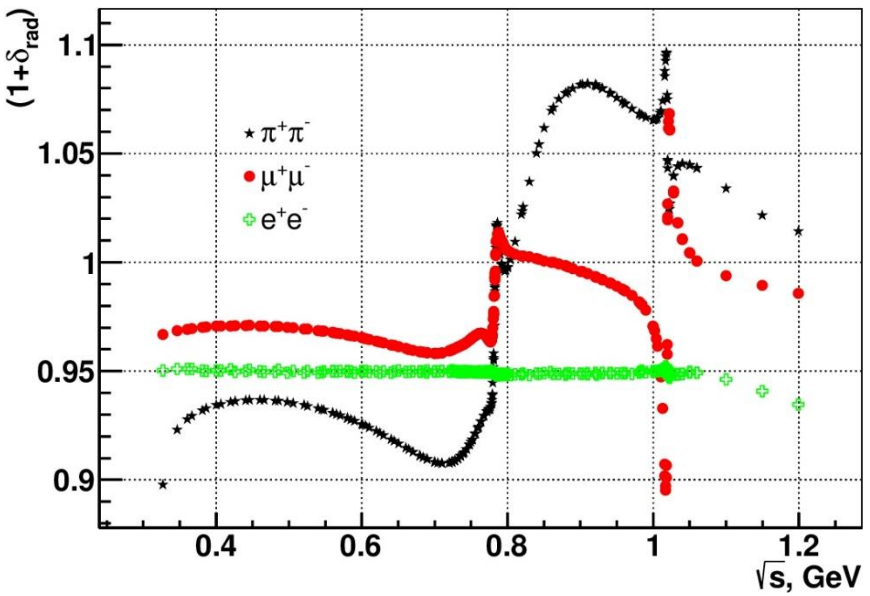

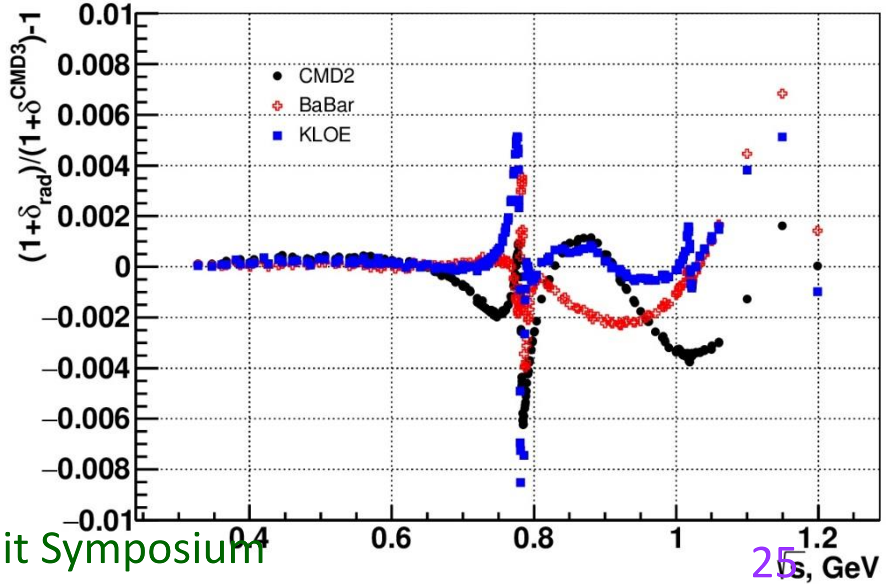

Forward-backward charge asymmetry

A = (N(θ < π/2) – N(θ > π/2))/N

Conventional sQED approach gives ~ 1% inconsistency
The theoretical model within GVMD was introduced,
describes well the CMD-3 data R.Lee et al., Phys.Lett.B 833 (2022) 137283
was confirmed by calculation in dispersive formalism
M.Hoferichter et al., JHEP 08 (2022) 295

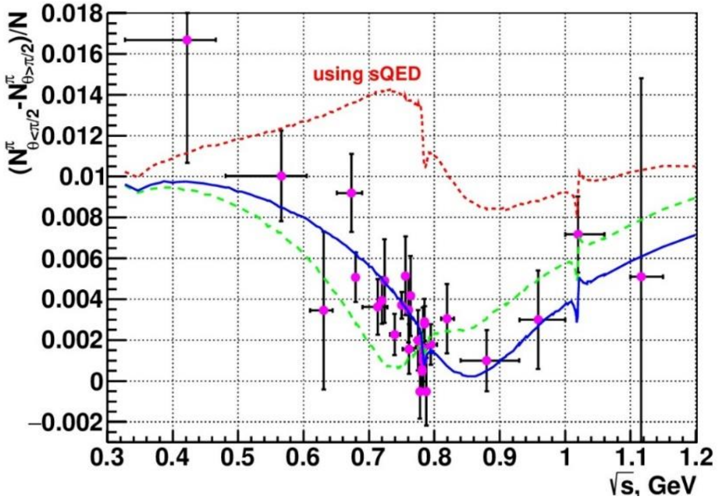

Scalar QED approach

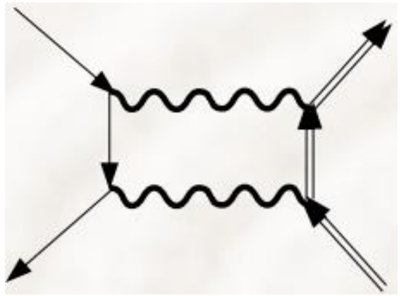

A = sQED*F(s)

Proper way

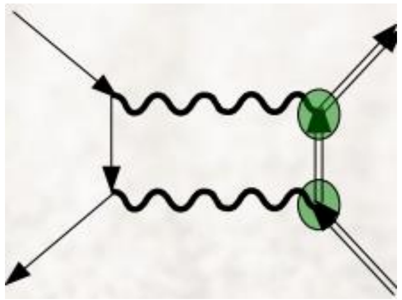

A ~ ∫F(q1)F(q2)

π+π-

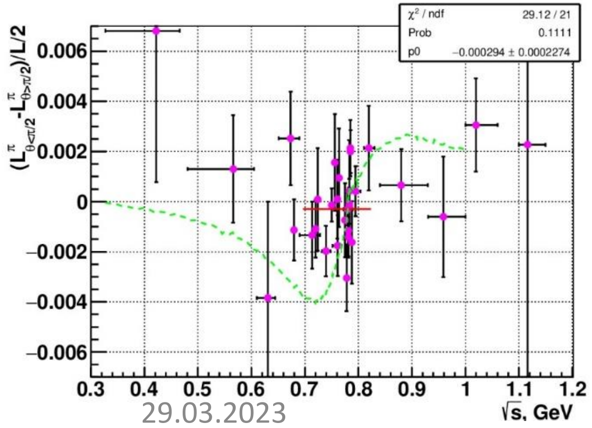

e+e-

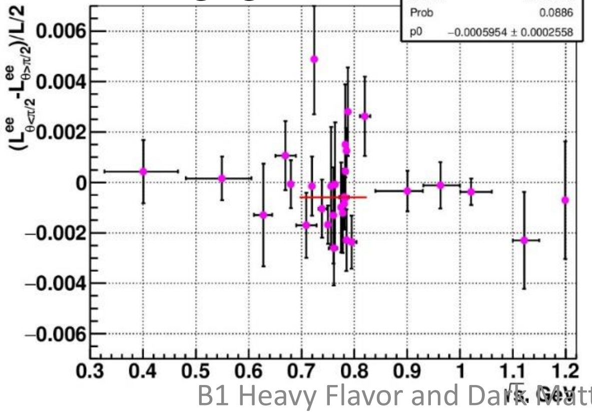

Thanks to Roman Lee
this calculations was done with above sQED

Consistency checks

Result consistent between seasons within < 0.1%

Mixed full MC data samples with detector conditioned over time
Same full analysis as for the data: efficiencies reconstructions, particle separation, etc same scripts, same intermediate files, etc
All underneath components (separation, efficiency reconstruction, etc) were checked with better precision

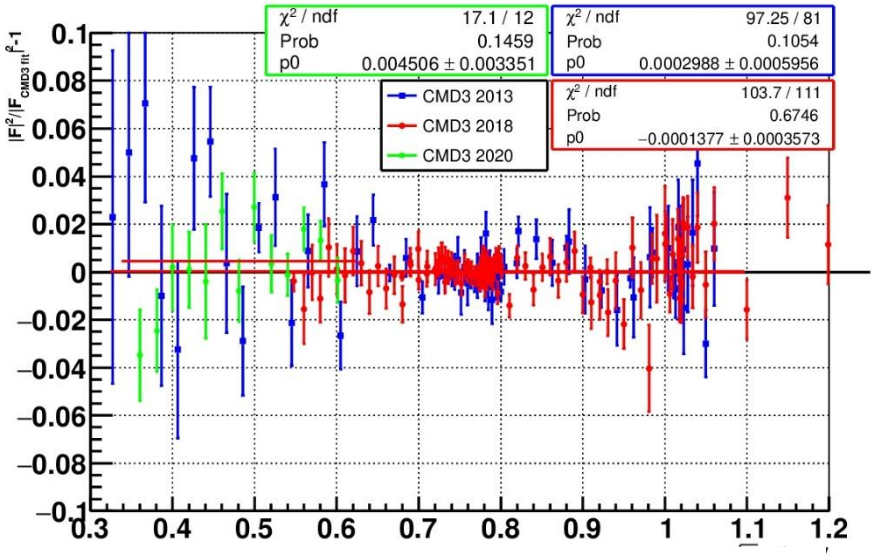

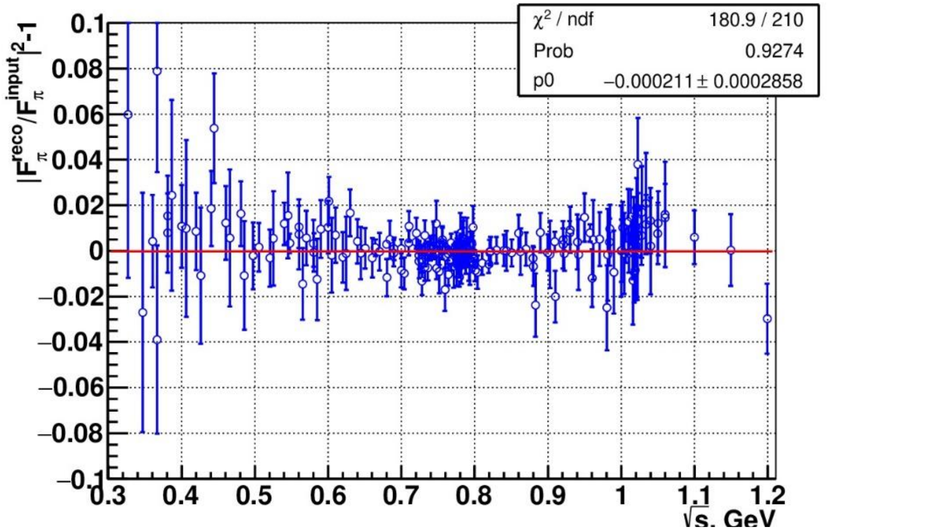

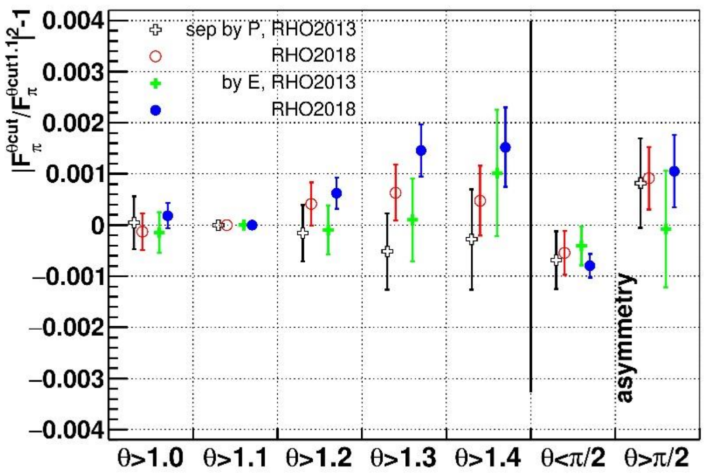

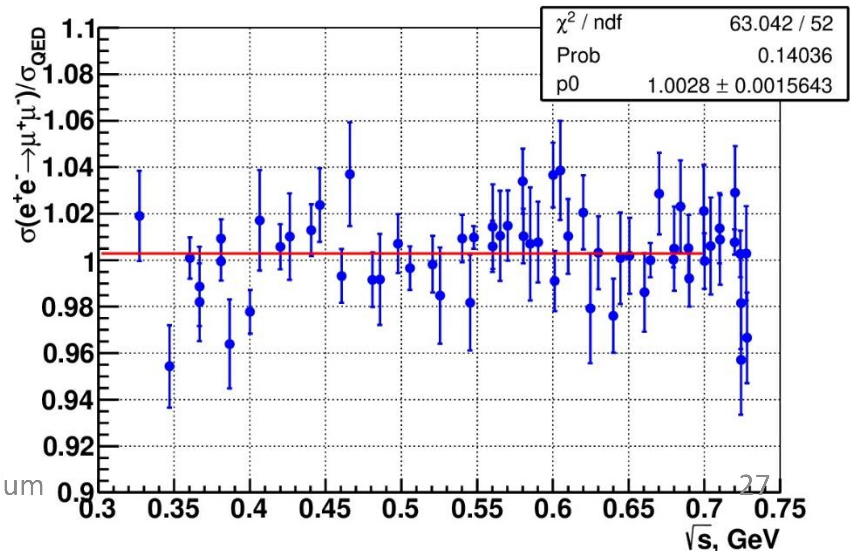

E vs P separatins

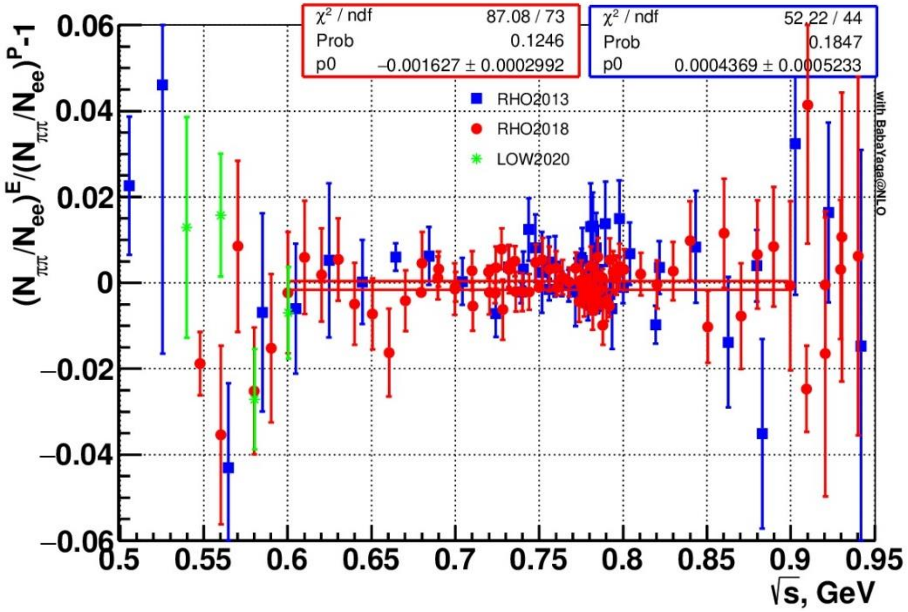

Fit by θ distribution

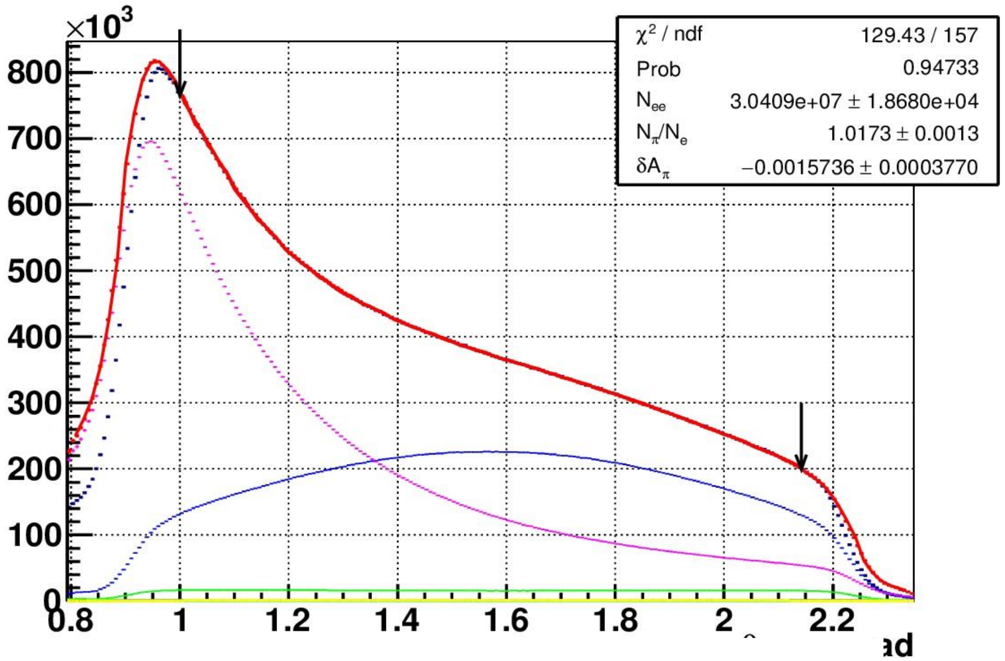

For sum of 350-410 MeV points
In comparison to the momenta separation
Δ (Nππ /Nee):
by energies in LXe Δ =(-0.089 +- 0.024)%
from theta with free δA: = (-0.20 +- 0.12)%
with fixed δA=0: = (+0.21 +- 0.07)%

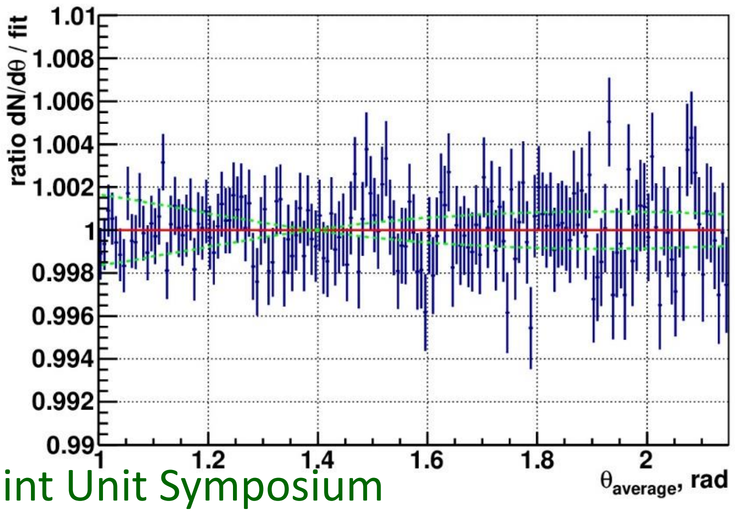

$|F_\pi|^2$ systematic uncertainty

Radiative corrections	0.2% (2π) ⊕ 0.2% (Fπ) ⊕ 0.1% (e+e-)
e/μ/π separation	0.5 (low) – 0.2 (ρ) – 0.6 (φ) %
Fiducial volume	0.5% / 0.8% (RHO2013)
Correlated inefficiency	0.1 (ρ) – 0.15%(>1 ГэВ)
Trigger	0.05 (ρ) – 0.3% (>1 ГэВ)
Beam Energy (by Compton σE< 50 keV)	0.1% (out of resonances), 0.5% (at ω, φ -peaks)
Bremsstrahlung loss	0.05 %
Pion specific loss	0.2% nuclear interaction
	0.2%(low) - 0.1% (ρ) - pion decay

Total **0.8% (low) – 0.7% (ρ) – 1.6% (φ)**

1.1% (low) – 0.9% (ρ) – 2.0% (φ) (RHO2013)

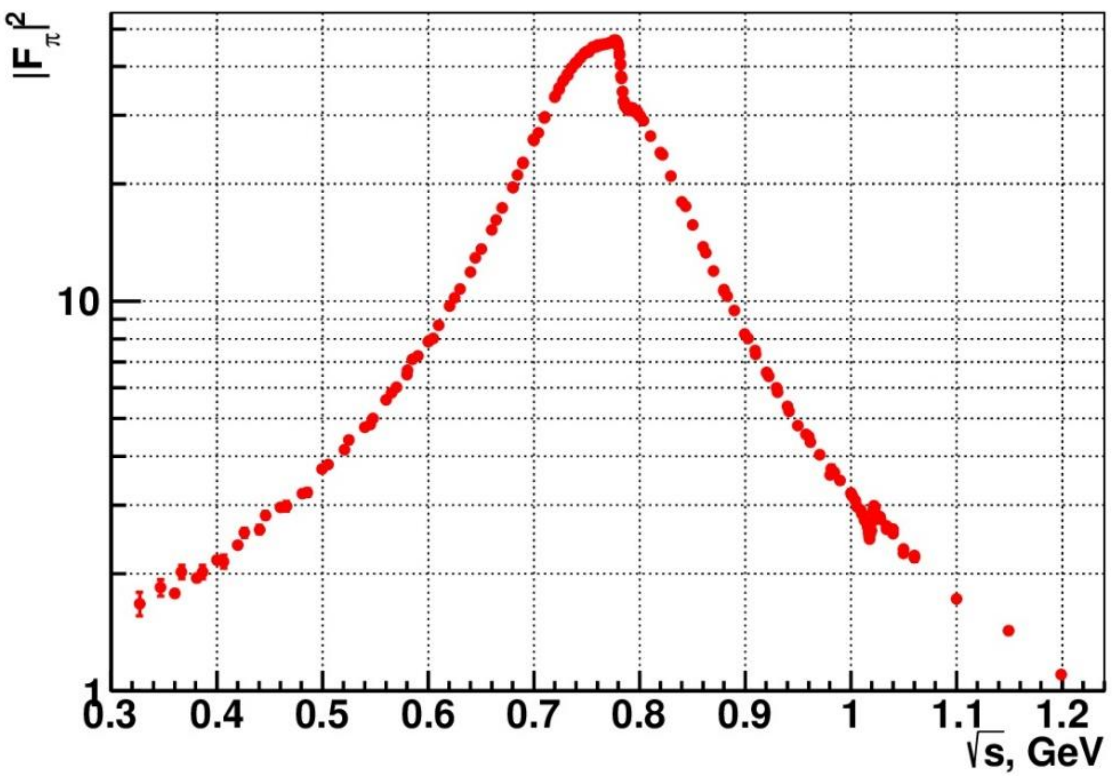

Results

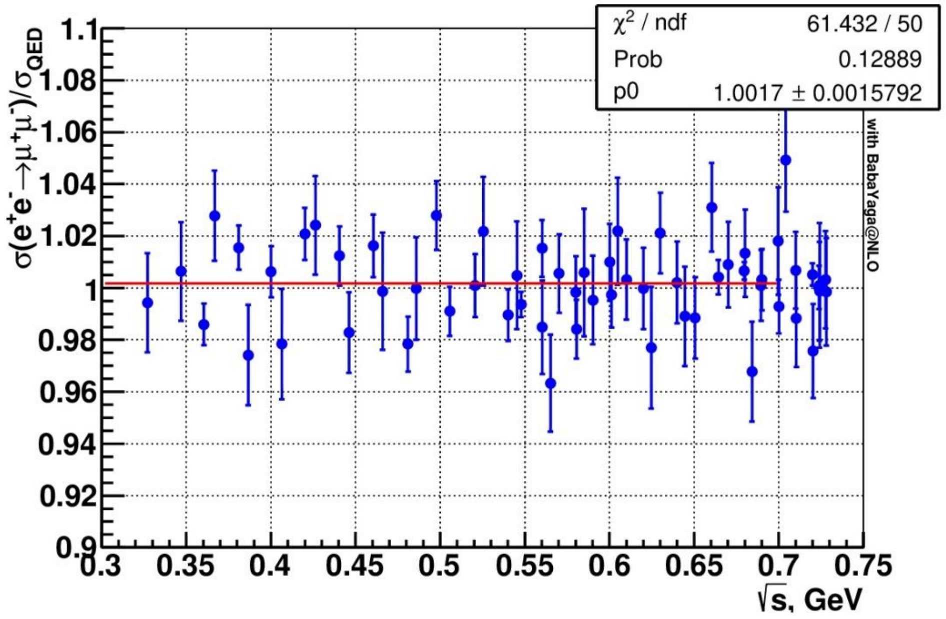

$$|F_\pi(s)|^2 =$$

$$|[GS_\rho(s)\cdot\left(1+\delta_\omega\frac{s}{m_\omega^2}BW_\omega(s)+\delta_\phi\frac{s}{m_\phi^2}BW_\phi(s)\right)+a_{\rho'}GS_{\rho'}(s)+a_{\rho''}GS_{\rho''}(s)+a_{cont}]/(1+a_{\rho'}+a_{\rho''}+a_{cont})^2$$

ρ, ρ', ρ'' - by the Gounaris-Sakurai parameterization (GS)
ω, φ - by the constant width relativistic Breit-Wigner
a_{cont} - constant for continuum contribution (partially absorb ρ', ρ'', ρ''' , …)
ρ', ρ'' – parameters fixed by combined fit together with CMD-2 and DM2, $\sqrt{s}$>1.1 GeV

Fit results

Parameter	value	$M_{\phi,\omega}, \Gamma_{\phi,\omega}$ constrained by PDG's values	PDG(2022) [61]
m_ρ, MeV	$775.41 \pm 0.08 \pm 0.07$	$775.4 \pm 0.07 \pm 0.07$	775.26 ± 0.23
Γ_ρ, MeV	$148.8 \pm 0.16 \pm 0.05$	$148.76 \pm 0.16 \pm 0.06$	147.4 ± 0.8
m_ω, MeV	$782.43 \pm 0.03 \pm 0.01$	$782.44 \pm 0.03 \pm 0.01$	782.66 ± 0.13
Γ_ω, MeV	$8.57 \pm 0.06 \pm 0.01$	$8.59 \pm 0.06 \pm 0.01$	8.68 ± 0.13
$\mathcal{B}_{\omega\to\pi^+\pi^-}\mathcal{B}_{\omega\to e^+e^-}, 10^{-6}$	$1.204 \pm 0.009 \pm 0.003$	$1.204 \pm 0.009 \pm 0.004$	1.28 ± 0.05
$\arg(\delta_\omega)$, rad	$0.167 \pm 0.008 \pm 0.01$	$0.169 \pm 0.008 \pm 0.012$	
m_ϕ, MeV	$1019.761 \pm 0.128 \pm 0.022$	$1019.465 \pm 0.016 \pm 0$	1019.461 ± 0.016
Γ_ϕ, MeV	$4.681 \pm 0.271 \pm 0.058$	$4.25 \pm 0.013 \pm 0$	4.249 ± 0.013
$\mathcal{B}_{\phi\to\pi^+\pi^-}\mathcal{B}_{\phi\to e^+e^-}, 10^{-8}$	$3.65 \pm 0.24 \pm 0.02$	$3.51 \pm 0.22 \pm 0.03$	2.2 ± 0.4
$\arg(\tilde{\delta}_\phi)$, rad	$2.883 \pm 0.052 \pm 0.011$	$2.77 \pm 0.023 \pm 0.006$	
$\lvert a_{cont} \rvert$	$0.0975 \pm 0.0011 \pm 0.0096$	$0.0971 \pm 0.001 \pm 0.0106$	
$\arg(a_{cont})$, rad	$2.337 \pm 0.021 \pm 0.286$	$2.344 \pm 0.02 \pm 0.309$	
χ^2/ndf	212.53 / 195	223.42 / 199	
m'_ρ, MeV	1226.22 ± 24.76		1465 ± 25
Γ'_ρ, MeV	272.97 ± 45.53		$400. \pm 60$
m''_ρ, MeV	1604.66 ± 30.8		1720 ± 20
Γ''_ρ, MeV	249.39 ± 52.24		$250. \pm 100$
$\lvert a'_\rho \rvert$	0.3589 ± 0.0693		
$\lvert a''_\rho \rvert$	0.1042 ± 0.031		
$\arg(a'_\rho)$, rad	-1.831 ± 0.07		
$\arg(a''_\rho)$, rad	3.384 ± 0.234		
χ^2/ndf	288.87/240		
CMD3+CMD2+DM2	$\chi^2 = 220.08(\text{CMD3}) + 25.30(\text{CMD2}) + 40.10(\text{DM2}) + 3.39(\text{PDG})$		
	ndf= $207+29+20+4 - 12(\rho, \omega, \phi, cont) - 8(\rho', \rho'')$		

$\phi\to\pi^+\pi^-$

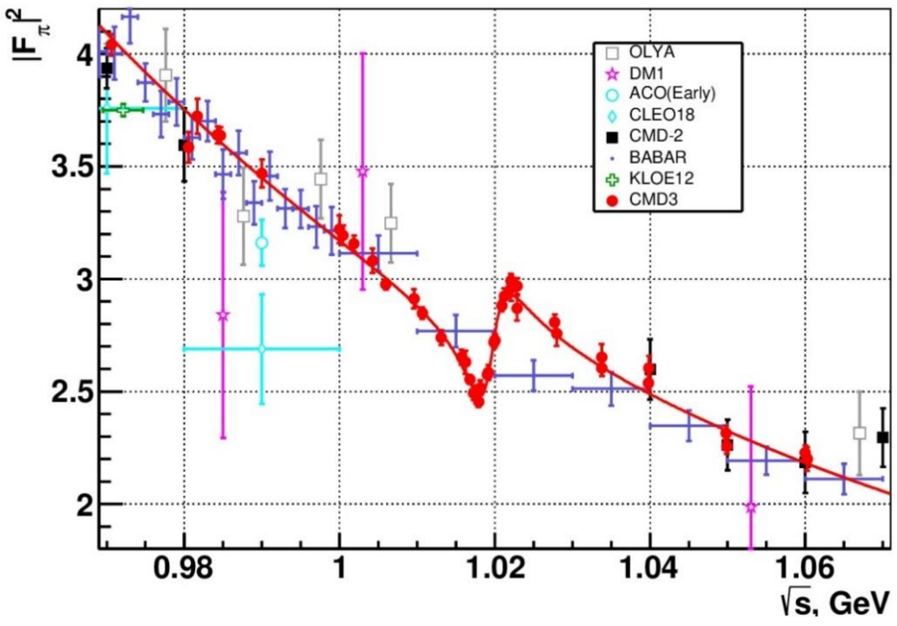

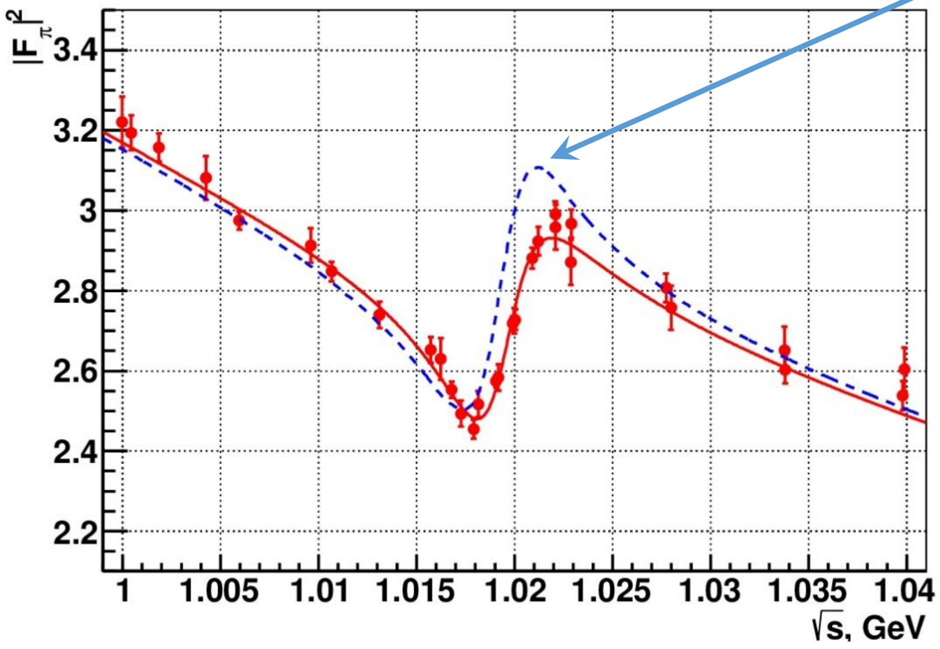

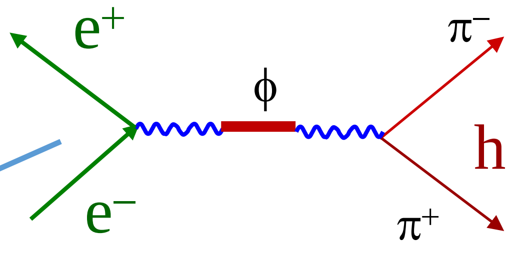

(BB)VP ~ 5.3x10^{-8}

$\Psi\pi$ = (-21.3 ± 2.0 ± 10.0)°

$B(\phi\to e^+e^-)B(\phi\to\pi^+\pi^-)$ = (3.51 ± 0.33 ± 0.24)x10^{-8}

Previous measurement using detected N$\pi+\pi$or visible cross-section by OLYA, ND, SND (Phys.Lett.B474:188-193,2000)

$\Psi\pi$ = (-34 ± 5)°

$B(\phi\to e^+e^-)B(\phi\to\pi^+\pi^-)$ = (2.1 ± 0.4)x10^{-8}

Comparison with other experiments

Relative to CMD-3 fit, green band – systematic value

vs direct scan

vs ISR

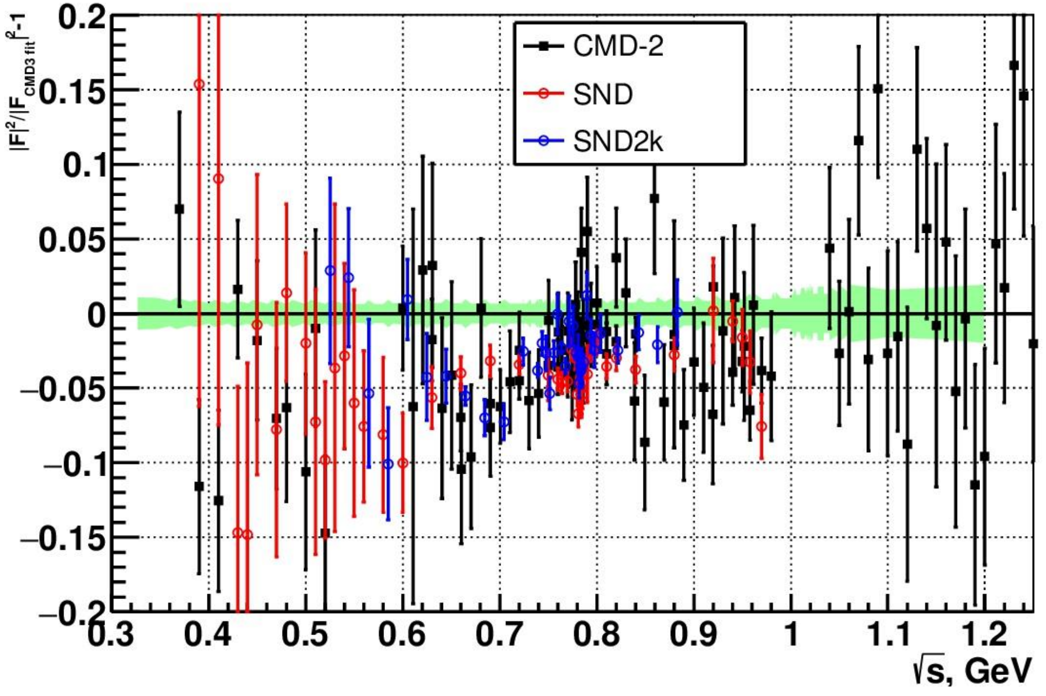

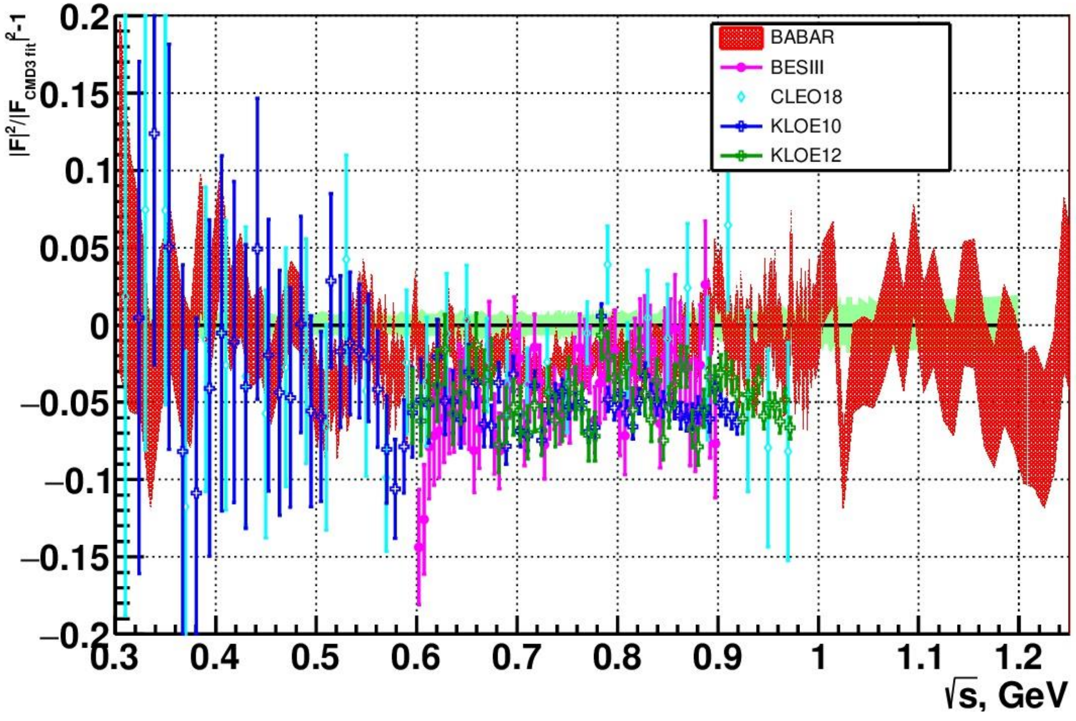

The contribution to a_μ^{had}

$$a_\mu^{had,LO} = \frac{m_\mu^2}{12\pi^3}\int_{4m_\pi^2}^{\infty}\frac{\sigma_{e^+e^-\to\gamma^*\to hadrons}(s)K(s)}{s}ds$$

$0.6 < \sqrt{s} < 0.88$ GeV

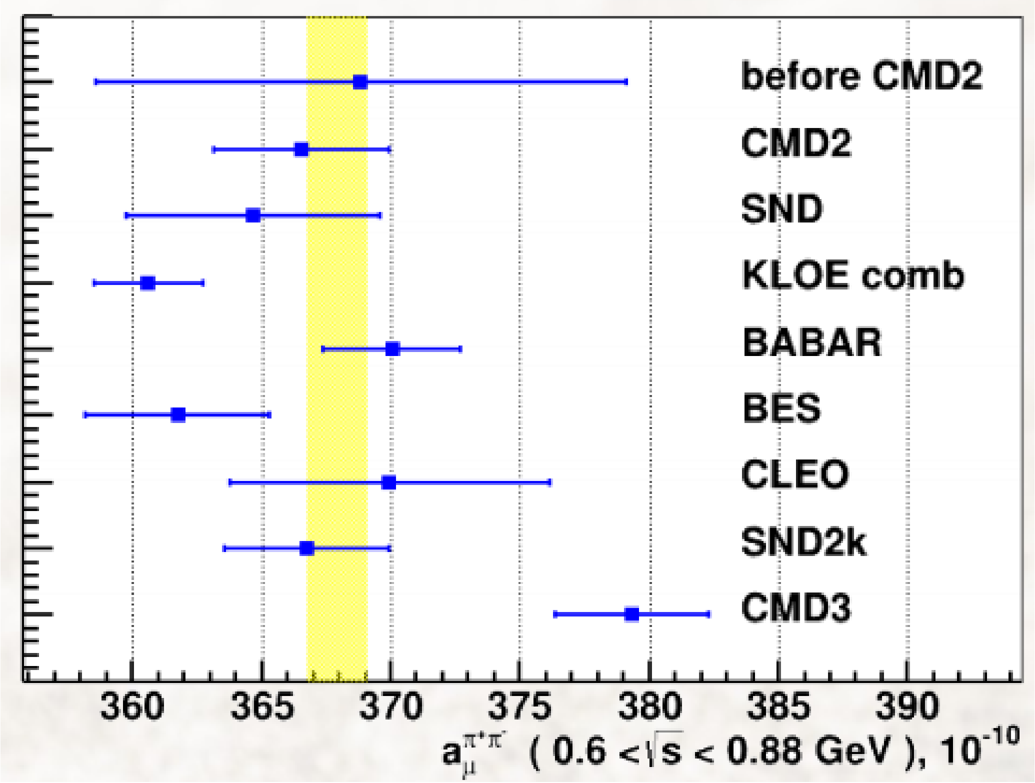

a_μ^{had},LO , 10^{-10}

before CMD2	368.8 ± 10.3
CMD2	366.5 ± 3.4
SND	364.7 ± 4.9
KLOE	360.6 ± 2.1
BABAR	370.1 ± 2.7
BES	361.8 ± 3.6
CLEO	370.0 ± 6.2
SND2k	366.7 ± 3.2
CMD3	379.3 ± 3.0

RHO2013 380.06 ± 0.61 ± 3.64
RHO2018 379.30 ± 0.33 ± 2.62
Sum 379.35 ± 0.30 ± 2.95 x10−10

Conclusion

CMD-3 pion formfactor measurement is based on full data set at $\sqrt{s} < 1$ GeV
34 x 10^6 of $\pi^+\pi^-$ events was used in analysis (at $\sqrt{s}<1$ GeV)

Total systematic uncertainty 0.7% / 0.9%(RHO2013)

VEPP-2000 collider is only one available now for direct energy scan below <2 GeV for measurements of hadronic cross section
We are thinking how to improve the precision of these measurements, which methods and instruments can help. All ideas are welcome!